Amyloid-β induced membrane damage instigates tunneling nanotubes by exploiting PAK1 dependent actin remodulation

Nandini Damodaran[1], Aysha Dilna[1], Claudia S. Kielkopf [2,3], Katarina Kagedal [2], Karin Ollinger [2] and Sangeeta Nath[1*]

[1] Manipal Institute of Regenerative Medicine, Manipal Academy of Higher Education, Bangalore, 560065, India.

[2] Experimental Pathology, Department of Clinical and Experimental Medicine, Linköping University, 581 85 Linköping, Sweden.

[3] Current address @ Illawarra Health and Medical Research Institute, University of Wollongong, Wollongong, New South Wales, Australia.

Abstract: Alzheimer's disease (AD) pathology progresses gradually via anatomically connected brain regions. The progressive pathology in AD is due to direct transfer of amyloid-β_{1-42} oligomers (oAβ) between connected neurons. However, the mechanism of transfer is not fully revealed. We observe that tunneling nanotubes (TNTs), nanoscaled f-actin containing membrane nanotubes, propagate oAβ and organelles directly from cell-to-cell. oAβ induced formation of TNTs are independent of cell type and differentiation stage of neuronal cells (SH-SY5Y). Preceding the formation, we detect oAβ induced plasma membrane (PM) damage and calcium-dependent repair through lysosomal-exocytosis and significant membrane surface expansion, followed by massive endocytosis to re-establish the PM. The massive endocytosis causes spontaneous internalization of oAβ via PAK1 (p21-activated kinase) dependent macropinocytosis and eventually accumulation in multi vesicular bodies/lysosomes. Moreover, formation of TNTs can be inhibited using small-molecule inhibitor IPA-3, a highly selective cell permeable auto-regulatory inhibitor of PAK1. The present study gives the insight that sprouting of TNTs instigate as consequences of oAβ induced PM damage and PAK1 dependent actin remodelling, probably to maintain cell surface expansion and/or membrane-tension in equilibrium.

Significance:

TNTs were recently discovered as a novel route in cell-to-cell pathology spreading of several diseases. Understanding the mechanism of direct cell-to-cell propagation of prion-like proteins has great implications in neurodegenerative diseases. Recent studies have shown that prion-like neurodegenerative proteins propagate via TNTs. Therefore, the mechanistic understanding that the involvement of PM repair via lysosomal-exocytosis and PAK1 dependent macropinocytosis and actin remodelling behind the formation of TNTs, has a pathophysiologic significance. The study reveals a new area on how stressed cells maintain homeostasis of intercellular communication by balancing exosome release and TNTs.

Short title: Direct cell-to-cell transfer of Aβ oligomers in TNTs.

Key words: Alzheimer's disease, Tunneling nanotubes, amyloid-β, lysosomal-exocytosis, p21 activated kinase dependent macropinocytosis, prion propagation.

Abbreviations.

AD - Alzheimer's disease.

oAβ - Oligomers of amyloid-β (1-42)

oAβ-TMR – Tetramethyl rhodamin labelled oligomers of amyloid-β (1-42)

PM- Plasma membrane

MVB – Multi vesicular body

PAK – p21-activated kinase

TNTs- Tunneling nanotubes

LAMP-1 - Lysosomal associated membrane protein-1

*** Corresponding to be addressed to sangeeta.nath@manipal.edu**

Introduction. Neurodegenerative diseases are propagating disorders characterized by accumulation of misfolded proteins that form aggregates, plaque and eventually cause neurodegeneration. Prion like self-propagation and gradual pathology progression (Prusiner, 2013) in a predetermined pattern to different parts of the brain is a common hallmark of neurodegenerative diseases. Several studies have shown that proteins involved in these diseases such as tau, Aβ, α-synuclein and huntingtin follow common patterns including misfolding, self-propagation and neuron-to-neuron transfer (Clavaguera *et al.*, 2009; Desplats *et al.*, 2009; Ren *et al.*, 2009; Ilieva, Polymenidou and Cleveland, 2009; Hansen *et al.*, 2011). In a model of Alzheimer's disease (AD), we have previously shown that spreading of AD pathology is due to direct transfer of amyloidogenic oligomers of Aβ between connected neurons (Nath et al., 2012). Moreover, lysosomal stress due to gradual accumulation of toxic non-degradable oAβ enhances the progression and the cell-to-cell transfer correlates with insufficient lysosomal degradation (Domert et al., 2014). Interestingly, transfer occurs much before the cells start to show detectable lysosomal toxicity (Domert et al., 2014). The studies (Nath et al., 2012; Domert et al., 2014) provided a possible explanations of how intracellular soluble oAβ reported as the potential initiator or driver of AD (Narasimhan *et al.*, 2017; Gouras *et al.*, 2010; Walsh and Selkoe, 2004), could develop gradual pathology by propagating between connected cells. However, mechanism of direct neuron-to-neuron propagation of neurodegenerative aggregates is not revealed yet.

Aβ induced neuronal dysfunction and impaired synaptic plasticity accountable for memory impairment is reported to be propagated to the neighboring cells (Kane *et al.*, 2000; Meyer-Luehmann *et al.*, 2006; Wei *et al.*, 2010). However, these studies did not reveal if such pathologic propagation is due to direct trans-synaptic transfer of toxic Aβ. In addition, exosomes are investigated as means of cell-to-cell transfer of Aβ (Rajendran *et al.*, 2006; Sardar Sinha *et al.*, 2018). However, these studies could not explain the anatomically connected strict spatiotemporal pathology progression of AD. On the other hand, cell-to-cell transfers of both extracellular and intracellular monomers and protofibrils of $A\beta_{1-42}$ via tunneling nanotubes (TNTs) are demonstrated in primary cultures of neurons and astrocytes (Wang et al., 2011). Recently, several studies have demonstrated TNTs to transfer neurodegenerative proteins, such as PrP^{Sc}, α-synuclein, Aβ, tau, polyQ, directly from one cell-to-another (Gousset *et al.*, 2009; Wang *et al.*, 2011; Zhu *et al.*, 2015; Tardivel *et al.*, 2016; Dieriks *et al.*, 2017). Several of these studies implicated links between TNTs and the endo-lysosomal pathway in cell-to-cell spreading (Bhat et al., 2018; Victoria and Zurzolo, 2017). These studies and the discovery of TNTs (Rustom et al., 2004) opened up a new direction in prion like cell-to-cell propagation in

neurodegenerative diseases. However, the molecular basis of TNTs formation remains underexplored.

TNTs are open ended membrane nano-structures with membrane actin protrusions between neighbouring cells. Correlative cryo-electron microscopy has recently demonstrated that TNTs are formed by 2-11 iTNTS and their diameters varies between 145 to 700 nm (Sartori-Rupp et al., 2019). TNTs are transient structures which stay intact for minutes to hours (Gerdes et al., 2013). Membrane protrusions like filopodium precede TNT formation and inhibition of actin polymerization attenuates its formation (Bukoreshtliev et al., 2009). TNT formation prevails in neuronal cells and primary neurons (Rustom et al., 2004). Successive studies also showed TNT formation in different cell types, such as immune cells, fibroblast, epithelial cells, astrocytes, neurons as well as their implication in the spreading mechanism of neurodegenerative diseases, HIV, HSV infections and in cancer (Onfelt *et al.*, 2004; Davis and Sowinski, 2008; Gerdes and Carvalho, 2008). A growing number of studies are trying to understand the mechanism behind the formation of TNTs. Some of these studies also reveal that vesicle transfer, recycling vesicles, lysosomes and molecule involved in membrane expansion play a role in the formation of TNTs, the actin membrane protrusions (Bhat et al., 2018; Victoria and Zurzolo, 2017; Hase et al., 2009). Actin depolymerization and actin modulations have been shown to inhibit the formation of these structures (Hanna et al., 2017).

In this study we show oAβ induced formation of TNTs and direct cell-to-cell propagation of oAβ between neighbouring cells. Preceding the formation of TNTs, we detect oAβ induced PM damage and repair through lysosomal exocytosis, membrane expansion and followed by massive endocytosis to re-establish the PM. The massive endocytosis causes spontaneous internalization of oAβ via PAK1 dependent macropinocytosis. Moreover, formation of TNTs can be inhibited by inhibiting PAK1 dependent macropinocytosis and actin remodulation. Altogether, these observations give new insights that sprouting of TNTs might be instigated as a consequence of oAβ induced PM damage and calcium dependent PM repair through lysosomal exocytosis via PAK1 dependent actin remodelling. This study also reveals the involvement of oAβ in inducing TNTs responsible for direct neuron-to-neuron transfer of amyloid pathology in AD progression.

Results.

oAβ induce cellular stress and formation of TNTs.

Cell-to-cell propagation of oAβ between connected cells have been shown in earlier studies (Wang *et al.*, 2011; Nath *et al.*, 2012; Domert *et al.*, 2014; Sardar Sinha *et al.*, 2018), however the clear mechanism still remains unexplained. Here, we image the uptake of oAβ in differentiated SH-SY5Y cells. We have observed that the internalization of 1 μM of oAβ-TMR (red) into early endosomes (Rab5 positive organelles) is followed by entry into multivesicular bodies (MVB) or lysosomes (Lamp1 positive organelles) after 1.5 h of incubation (Figure 1A). Extracellularly applied oAβ-TMR (200 nM to 1 μM verified) was internalized efficiently within 15 min and quantification showed that 60-82 % of oAβ-TMR ended up in Lamp1 positive organelles (results not shown). Morphologically, these cells exhibit blebs and noticeable cell membrane expansion as well as nanotubes between neighbouring cells. Here, we show images of cells incubated for 3 h with 500, 250 and 100 nM of oAβ-TMR (Figure 1B, (Supplementary Movie 1-3). The lengths of the TNTs were between 0.2-16 μm (marked with white boxes, Figure 1B). We did not observe significant numbers of TNT like structures and unusual membrane expansions in the differentiated control cells (Figure 1C). We quantified the number of cells with unusual blebs/lamellipodia and TNTs with respect to the total number of cells and found a concentration dependent increase, when quantifying oAβ-TMR treated cells (200-500 nM) compare to the control cells (Figure 1D, E).

In order to show that the studied TNTs structures are not dependent on neuronal cell differentiation stages, we performed the experiments in partially differentiated SH-SY5Y neuronal cells, treated with retinoic acid (RA) for 7 days, as well. We have observed thin TNTs extended from expanded lamellipodia-like membrane protrusions in partially differentiated SH-SY5Y cells internalized with oAβ-TMR after incubation with 250 nM of oligomers for 3 h (Figure 1F-G). Moreover, the partially differentiated SH-SY5Y cells form networks of TNTs between neighbouring cells (Figure 1G). The cells make networks between 3 neighbouring cells via TNTs (white arrows), and those TNTs were also extended from expanded lamellipodia (black arrows, Figure 1F). We have also quantified oAβ-TMR induced cells with unusual blebs/lamellipodia and TNTs in partially differentiated cells treated with 250 nM of oAβ-TMR for 3 h (Figure 1I), compare to the control cells (Figure 1H). The results showed increased number of cells with blebs/lamelliopodia and TNTs when incubated with oAβ-TMR compared to controls.

TNTs propagate oAβ and organelles from one cell-to-another.

We have followed transfer of oAβ-TMR (white arrows, Figure 2A, Supplementary Movie 1) via TNTs from one cell-to-another in differentiated cells by time-laps imaging. We have also observed TNTs extended from expanded lamellipodia (indicated by black arrows) and transfer of oAβ-TMR colocalized with Lysotracker labelled lysosomes to the connected neighbouring cells (white arrow, Figure 2B). Differentiated cells form neurites and in our previous studies we have extensively characterized neuronal properties of those cells (Agholme *et al.*, 2010; Nath *et al.*, 2012). Differentiated control cells form numerous networks of neurites, stained with early endosomal marker Rab5 (green) and mitotracker (red) (Figure 2C). oAβ is toxic to the neurites of differentiated cells and the neurites get degraded over the time and with increasing concentrations of oligomers treatment (Supplementary Figure 1). On the other hand, the numbers of TNT formation depends on the concentration of oAβ. Degradation of neurites are not significant at 100 nM of oAβ incubated for 3 h. Instead, formation of few TNT like structures extended from lamellipodia are distinctly visible at this condition (Marked with T in the Supplementary Movie 3). We have also observed propagations of organelles via TNTs extended from lamellipodia in differentiated cells treated with 250 nM of oAβ for 3 h (Supplementary Movie 2). At 250 nM, the healthy neurites are fewer in numbers and membrane of the cells are often expanded with blebs or lamellipodia (Supplementary Movie 2). Differentiated cells after 6 h incubation with oAβ frequently show TNT-like thin connections direct from one cell-to-another, with early endosomal marker rab5 (green) and mitotracker (red) labelled organelles (Figure 2C). However, neurites get degraded by oAβ incubation in a time and concentration dependent manner. Toxicity studies were also performed with 1 μM of oAβ over the days and results show gradual degradation of neurites over the time, however the XTT assay cannot not detect any significant cell death (Supplementary Figure 1).

oAβ induced TNT formation precedes enhanced membrane activities and massive endocytosis.

We have designed the experiments using undifferentiated (SH-SY5Y) cells to ensure that it is the toxicity of oAβ causes induction of TNT like structures, not the differentiating reagents. As presented in Figure 3A, undifferentiated SH-SY5Y cells incubated with 1 μM of oAβ together with the membrane impermeable dye TMA-DPH form TNTs within 10 min. Moreover, the oAβ induced TNT formation precedes the enhanced membrane activities along with the formation of membrane ruffles, filopodium, blebs and massive endocytosis process as compared to the control cells (Figure 3A; Supplementary Movie 4,5). The oAβ-induced

massive endocytosis was quantified by measuring the internalized TMA-DPH from the luminal part of the cells (Figure 3B). Immediate addition of oAβ instigates threads of membrane extensions between two neighbouring cells and the membrane threads were not developed on the bottom of the dishes, rather they formed as suspended structures without attaching to substratum (Supplementary Movie 6). On the other hand, the membrane impermeable dye TMA-DPH is able to enter the cells treated with oAβ (1 μM) for 1 h, as the dye stain the cells completely and immediately at the addition (Figure 3C). The result suggests oAβ induced change in the membrane fluidity.

To understand if the oAβ induced TNT formation is specific to neuronal cells or if it is a basic cellular process, we incubated HEK-293 cells with oAβ (1 μM) for 1 h and we have observed formation of long TNTs hanging between distant neighbouring cells (Supplementary Figure 2C). Similar to SH-SY5Y cells, the cell membrane in the control HEK-293 cells was observed to be labelled by TMA-DPH only at the periphery. In contrast, in the oAβ (1 μM for 1 h) treated HEK-293 cells, TMA-DPH leached immediately into the cells and those cells also showed TNT protrusions (Supplementary Figure 2A-B). The results are also nullifying any probability of artefact of neurite-like protrusions in SHSY5Y cells and indicating oAβ induced protrusions are TNTs.

oAβ$_{1-42}$ induces membrane damage and lysosomal exocytosis.

oAβ induces TNT formation in association with the substantial enhancement of membrane activities and massive endocytosis, similarly as evident in Ca^{2+} dependent repair of injured PM by lysosomal exocytosis (Idone et al., 2008), inspired us to determine if oAβ caused PM damage. The Gold standard to detect PM repair by lysosomal exocytosis and formation of a patch over the damage membrane is to detect the luminal part of the lysosomal membrane protein LAMP-1 exposed on the outer leaflet of the plasma membrane. Accordingly, we have observed oAβ (1 μM) induced Lamp1 on the PM, in undifferentiated SH-SY5Y cells within 15-30 min of exposure (Figure 3D, E). To verify that the process is calcium dependent, we analysed influx of the membrane-impermeant dye propidium iodide (PI) in presence of 5 mM EGTA in PBS. The rationale behind this experiment is that if lysosomal exocytosis-dependent PM repair is occurring, chelation of Ca^{2+} will prevent the repair and PI will be detected intracellularly. As seen in Figure 3F-H, significant enhancement of PI staining was detected within 30 min to 2 h after exposure to oAβ as quantified by flow cytometry and confocal imaging. Thus, we conclude that addition of 1 μM of oAβ causes damage to the PM and as a

membrane repair process, lysosomal exocytosis and fusion of lysosomal membrane with the PM occur. Subsequent to the membrane repair process, re-establishment of the PM occurs by removing membrane parts through endocytosis and as a consequence, oAβ is internalized into endosomes (Rab5 positive) followed by entry into lysosomes (Lamp1 positive) (Figure 1A).

PAK1 dependent macropinocytosis is involved in massive internalization of oAβ$_{1-42}$.

We next wanted to understand the exact mechanism of the massive internalization of oAβ. To identify the mechanisms of massive internalization of oAβ-, partially differentiated SH-SY5Y cells were pre-treated with different inhibitors against uptake mechanisms which are suggested by the literature to be relevant for Aβ-uptake. We have used partially differentiated cells, because N-methyl-D-aspartate (NMDA) receptors, a-amino-3-hydroxy-5-methyl-4-isoxazolepropionic acid (AMPA) receptors and nicotinic acetylcholine receptors (nAChR) are known to be present on RA treated partially differentiated SH-SY5Y cells (Xie et al., 2010) and were shown to mediate the internalization of Aβ (Bi et al., 2002; Zhao et al., 2010; Yang et al., 2014). To inhibit the function of these receptors, antagonists against NMDA receptors (AP-5), AMPA receptors (GYKI 52466) and nAChR (α-Bungaratoxin) were used and oAβ uptake was quantified by flow cytometry. Inhibitors of receptors showed no change in the uptake of oAβ (Figure 4A).

Aβ is also known to be taken up by endocytosis, both clathrin-, dynamin-dependent and as well as clathrin-, dynamin-independent pathways. Furthermore, various reports on internalization of Aβ aggregates in neurons primarily showed that uptake depends on lipid rafts and lipid rafts associated receptors, some reports have also implicated a lipid rafts independent process. Variable reports of uptake mechanism could be due to different aggregates in terms of toxicities and conformations (McLaurin and Lai, 2011). Therefore, we have studied internalization using different endocytic inhibitors to attenuate these processes; DPA, which functionally inhibits acid sphingomyelinases (Kornhuber et al., 2011); bafilomycin A1 (Baf), which inhibits autophagy at late stage by inhibiting vacuolar ATPases and lysosome acidification; NH_4Cl which lowers the pH of intracellular vesicles which leads to inhibition of endosomal maturation by inhibiting vesicles fusion (Poëa-Guyon et al., 2013) and thereby also attenuates exocytosis; MDC is an inhibitor of clathrin-mediated endocytosis as it inhibits the tissue transglutaminase which mediates clustering and internalisation of clathrin (Guo et al., 2015); PAO also inhibits clathrin-mediated endocytosis through a mechanism not fully elucidated (Gibson et al., 1989); while dynasore is a dynamin inhibitor which blocks the formation of coated vesicle formation

during endocytosis (Macia et al., 2006). Furthermore, Aβ was earlier shown to be taken up by macropinocytosis in microglia and astrocytoma cells (Mandrekar et al., 2009; Li et al., 2014). IPA-3 can inhibit macropinocytosis by regulating Pak1 (Deacon et al., 2008) and EIPA through inhibition of Na^+/H^+ exchangers (Mercer and Helenius, 2009). After pre-treatment with the inhibitors, the cells were treated with oAβ-TMR and quantified by flow cytometry (Figure 4B-C). The percentage of oAβ-positive cells was normalized to the mean percentage of Aβ-uptake to calculate the fold-change upon inhibitor treatment. Internalization of oAβ was inhibited consistently with significance by NH_4Cl and IPA-3. Inhibition by Baf was significant, however, there were variations in batches (Figure 4B-C). NH_4Cl can inhibit the uptake in general by inhibiting fusion of endosomal vesicles and exosomes. But inhibition by IPA-3 (~ 50 %) suggests the role of PAK1 dependent macropinocytosis. To establish if the oAβ internalization in undifferentiated SHSY5Y cells occur similarly via PAK1 dependent micropinocytosis, we have also quantified the internalization of oAβ in undifferentiated SH-SY5Y cells using NH_4Cl, Baf and IPA-3 (Figure 4D). The quantification showed similar results as in partially differentiated cells, the representative confocal images of internalization in undifferentiated cells were shown in Figure 4D.

IPA-3 inhibits the formation of TNTs by inhibiting PAK 1 dependent actin remodulation. TNTs are nanoscaled f-actin containing open ended membrane protrusions between two neighbouring cells. Actin depolymerizing drugs latrunculin and cytochalasin impair TNTs formation (Rustom et al., 2004). Activation of PAK1 regulates cortical actin polymerization, directional movements and also polarized lamellipodia at the leading edge (Sells et al., 1999). Therefore, the next logical step was to observe if inhibition of oAβ uptake by IPA-3, an inhibitor of PAK1 dependent macropinocytosis, can also inhibit the formation of TNTs. To do so, SH-SY5Y cells were transfected using lifeact-EGFP plasmid (Figure 5A) and CAAX-mCherry plasmid (Figure 5B), to stain f-actin and peripheral membrane proteins, respectively. Images from fluorescence microscopy was used to follow the number of labelled TNTs quantitatively (Figure 5A-C). Cells that have been co-transfected with lifeact-EGFP and CAAX-mCherry, showed co-stained TNTs, indicating that these TNTs are continuous extension of the PM and actin protrusions between two cells (Figure 5B). As observed in non-transfected cells, the increased number of TNTs formed in oAβ treated cells as compared to the controls maintained. Cells that were treated with IPA-3, a known PAK1 inhibitor, showed a decreased number of TNTs (Figure 5A, C). Morphologically, IPA-3 treated cells were more rounded than the controls and oAβ treated cells. The percentage of TNTs was calculated and

plotted as a bar graph, which indicating that oAβ treated cells showed an increase in the number of TNTs formed, hence confirming that cellular stress caused by the build-up of aggregates or due to the PAK1 dependent rapid-internalization process might cause the formation of TNTs.

Superresolution imaging reveals PAK1 inhibitor IPA-3 dependent remodulation of f-actin.

Superresolution SIM (Structured Illumination Microscopy) images were obtained using DeltaVision™ OMX SR microscopy (Fig 6). We were able to observe the lifeact EGFP plasmid labelled f-actin structures at a resolution of < 130 nm. Distinct differences in f-actin structures between oAβ treated and the oAβ + IPA-3 treated cells were observed. TNTs were observed to be continuous extension of long cortical f-actin in oAβ treated cells (Figure 6A and $A^{/}$). 3D volume view of the xyz-plane clearly demonstrated that membrane actin protrusion did not grow on the surface like neurites. Rather, they were 'hanged' between two neighbouring cells, as one of the characteristics features of TNTs (Figure $6A^{//}$). oAβ treated cells showed numerous long f-actin structures as part of the membrane cortex and also bunch of long f-actin extensions similar to the actin organizations of polarized lamellipodia (Figure 6B). In contrast, in the IPA-3 pretreated cells there were disruptions observed in the actin fibres, which could indicate that PAK1 has an important role in actin modulation and hence in TNT formation (Figure 6C). Additionally, the formation of branched actin and inhibition of oAβ induced TNTs in IPA-3 pretreated cells was clearly observable by wide-field images taken by fluorescence microscope (Supplementary Figure 3).

oAβ propagation to healthy cells is mediated by transport in TNTs.

To study how cells with accumulated endogenous oAβ transfer the material to neighbouring healthy cells, we have used a 3D donor-acceptor co-culture model that we have designed and used previously to show cell-to-cell direct transfer of oligomers and pathology spreading (Nath *et al.*, 2012; Domert *et al.*, 2014). As acceptor cells, differentiated SH-SY5Y cells transfected with EGFP-tagged endosomal protein (green, Rab5a) were used, while the donor cells were incubated with oAβ-TMR (red). In our previous work (Nath et al., 2012), we showed transfer of oAβ-TMR donor (red) to acceptor cells (green) using images captured by time laps recording. However, we did not show if acceptor cells that had internalized oAβ-TMR can further transfer oligomer to the next acceptor cells. Here, we show that acceptor cells (1) that contained oAβ transferred by the donor cells formed TNT-like, thin membrane extensions (white arrows) towards healthy differentiated acceptor cell and transferred oAβ (yellow arrow)

to the acceptor cell 2 (Figure 7A). Additionally, the oAβ-TMR containing acceptor cells form transient filopodium like structures and blebs, which are not detected in matured differentiated neuronal controls. Acceptor cells that have no transferred oAβ-TMR appear healthy as judged by appearance of neurites and no significant blebs / lamellipodia (Figure 7A). Noticeably, stressed cells form TNTs like transient membrane protrusions towards healthy one within 24 h (Figure 7A). The cells accumulated with transferred oAβ gradually develop lysosomal pathology (Domert et al., 2014 and Figure 7B). Eventually, the accumulation of non-degradable oAβ-TMR in Lamp1 positive MVB/lysosomes causes gradual development of extra-large lysosomes over 48 and 72 h and the intracellularly accumulated oligomers can also induce TNTs like protrusions (Figure 7B, white arrow). We have already reported in our earlier study (Domert et al., 2014) that lysosomal stress develops gradually by accumulated oligomers which is significantly detectable after 48 h. Gradual lysosomal pathology development and appearance of blebs / lamellipodia and TNTs were quantified by counting the images of acceptor cells transferred with oligomers and donor cells (Figure 7C-D). Donor cells as well as acceptor cells accumulated with oAβ-TMR showed significantly more blebs/lamellipodia and TNTs than control cells. DIC (differential interference contrast microscopy) imaging using confocal microscope is not an ideal method for capturing of nano-scale TNTs structures, especially in a 3D co-culture cellular model. Thus, there is a risk of under estimation in quantification.

Discussion. Prion like cell-to-cell propagation is a common characteristic of neurodegenerative diseases. Several reports have consistently reported direct cell-to-cell propagation of neurodegenerative protein aggregates and their implications in the gradual pathology progression (Clavaguera *et al.*, 2009; Desplats *et al.*, 2009; Ren *et al.*, 2009; Ilieva, Polymenidou and Cleveland, 2009; Hansen *et al.*, 2011). Our previous work has shown that, in AD gradual pathology progression is due to direct transfer of intracellularly accumulated non-degradable soluble oAβ (Nath *et al.*, 2012; Domert *et al.*, 2014). However, the mechanism of cell-to-cell propagation is unexplored. Synaptic transfer has been investigated as a potential mechanism. Aβ induced spine loss and impaired synaptic plasticity are early pathologies and develop before neurodegeneration (Wei et al., 2010). Moreover, Aβ causes disruption of the synaptic transmission mediated by the synaptic receptors NMDA and AMPA (Walsh and Selkoe, 2004; Venkitaramani *et al.*, 2007). Therefore, neuron-to-neuron synaptic transmission of oAβ is unlikely. Likewise, inhibition of the possible receptors involved in synaptic

transmission did not show any effect on the cell-to-cell transfer of Aβ in the cultured differentiated neuronal cells (Nath et al., 2012). Moreover, an increased number of reports show that cell-to-cell transfer of common neurodegenerative proteins, such as PrP^{Sc}, α-synuclein, tau, polyQ aggregates and Aβ, via TNTs instigate new avenues (Gousset *et al.*, 2009; Wang *et al.*, 2011; Zhu *et al.*, 2015; Tardivel *et al.*, 2016; Dieriks *et al.*, 2017).

Aβ peptides are mainly generated extracellularly from transmembrane amyloid precursor protein (APP) by β- and γ-secretase enzymatic cleavage. Recent studies have shown the presence of β- and γ-secretase machineries and APP at the membranes of endo-lysosomes and generation of Aβ peptides in the lumen of endosomes and lysosomes (LaFerla, Green and Oddo, 2007; Gouras *et al.*, 2010; Edgar *et al.*, 2015). Increasingly, clinical studies and animal models indicate that soluble oAβ is the disease initiator and driver, rather than large extracellular depositions. Importantly, it was recently reported that the intracellular pool is mainly formed from aggregation-prone, toxic Aβ42, while the less toxic Aβ40 is more abundant extracellularly (Sannerud et al., 2016). Intracellular accumulation of amyloidogenic proteins causes decreased lysosomal efficiency, detected as reduced capacity of degradation, abnormal lysosomal morphology and lysosomal membrane permeabilization as hallmark of neurodegenerative diseases (Freeman *et al.*, 2013; Eriksson *et al.*, 2017;Victoria and Zurzolo, 2017; Gowrishankar *et al.*, 2015). Lysosomes are central hubs for nutrient homeostasis but are also actively involved in cell death induction and PM repair. Stress signals from lysosomes also induce various signals affecting mitochondria and the nucleus. Furthermore, these stress signals dysregulate various cellular processes and mediate increased oxidative stress (Appelqvist *et al.*, 2013; Ditaranto, Tekirian and Yang, 2001; Eriksson *et al.*, 2017; Freeman *et al.*, 2013). Several studies have indicated that ROS (reactive oxygen species) induced cellular stress enhances TNT formation (Rustom, 2016). Notably, lysosomal stress as well as damage due to accumulation of non-degradable amyloidogenic aggregates could induce formation of TNTs (Abounit et al., 2016) and cell-to-cell transfer of oAβ, which correlates with insufficient degradation efficiency of lysosomes (Domert et al., 2014).

In contrast, impaired processing of Aβ due to lysosomal enzymatic inefficiency and enhanced exocytosis was demonstrated by Annunziata *et al.*, 2013. Additionally, the study by Hase *et. al.* 2009 also reported that M-sec, a related protein of the exocyst complex involved in exosome fusion and membrane expansion, regulates formation of TNTs. PM recruitment of Ral-GTPase and filamin, both actin remodeling proteins, also indicate positive regulating effects in TNT formation (Hase et al., 2009). The study presented here also demonstrates unusual membrane expansion in the form of blebs, filopodium-like structures and extension of TNTs from

expanded membranes. Upregulation of the exocyst complex during TNT formation might be prearrangement of rapid exocytosis as a Ca^{2+}dependent membrane repair process. Exocyst complex is also overlapped with endosomal trafficking, both pathways are associated with vesicular transports from golgi to PM (Chen et al., 2008). Previous reports have indicated that synthetic oAβ makes ion-permeable pores in synthetic membranes (Arispe, Pollard and Rojas, 1993; Kagan, 2012). Recently, it was also shown that oAβ can induce a membrane repair response similar to that induced by exposure to the bacterial pore-forming toxin produced by *B. thuringensis* (Julien *et al.*, 2018). Consequently, enhanced internalization of Aβ occurs via endocytosis, which is independent of receptor interactions.

Internalization of the oAβ pool appears to occur via early endosomes and is directed to lysosomes, where non-degradable, aggregation-prone oAβ gradually induces lysosomal stress. Notably, propagation of amyloidogenic seeds is observed much earlier, whereas lysosomal pathology develops gradually over time (Domert et al., 2014). Involvement of the clathrin- and dynamin-independent endocytosis is also relevant in maintaining cellular homeostasis by regulating membrane stress and cell surface expansion (Apodaca, 2017; Thottacherry *et al.*, 2018). Recent study reported that induced macropinocytosis could be the cause of decreased plasma membrane stress (Loh et al., 2019). Exocytosis is involved in the expansion of cell surface area and results in decreased membrane stress. Reduced membrane stress also arises during PM repair, due to extensive exocytosis events (Andrews and Corrotte, 2018). Endosomes recycling also plays a big role in maintaining membrane surface area in equilibrium (Grant and Donaldson, 2009). Interestingly, the role of vesicle recycling in TNT formation has been evaluated in a recent study carried out on CAD cells, where increased level of Rab 11a, Rab 8a and VAMP3 were reported in correlation to TNT-connected cells (Bhat et al., 2018).

We have observed the formation of TNT networks between three cells and also thread like membrane continuity hanging between two neighbouring cells before emerging as long membrane protrusions, the observations were also demonstrated previously where TNTs were shown as a mode of intercellular cell communication (Rustom et al., 2004). We have characterized the oAβ induced TNT like structures as their capacity to stay hanged between two cells, even in the paraformaldehyde fixed cells, without touching the surface of the cultured dish. Altogether, our results have been established that, TNTs are characteristically membrane actin protrusions connecting the two neighbouring cells ‘hung’ between two neighboring cells in response to rapid membrane repair and cell surface expansion, probably to maintain the membrane stress in equilibrium.

The results of oAβ internalization have clearly shown that the massive endocytosis is clathrin and dynamin-independent, but rather follows a Pak1-dependent macropinocytosis pathway. Macropinocytosis is an actin dependent process where cells engulf and take up fluids and membranes into intracellular vesicles referred to as macropinosomes, which then mature into late endosomes/MVB. It has been shown that PAK1 specifically regulates macropinocytosis by following the uptake of 70k Da dextran in mutant strains of PAK1(Dharmawardhane et al., 2000). PAK1 is a serine/threonine kinase found in the cytoplasm and nucleus of cells and PAK1 is important in regulating cytoskeleton remodelling, phenotypic signalling, gene expressions and it affects a variety of cellular processes (Sells et al., 1999). In addition, PAK1 acts downstream of the small GTPases Cdc42 and Rac1, which interact with many effector proteins, including Arp2/3, which in turn can have an effect on cytoskeleton reorganization (Daniels et al., 1998). PAK1 has an autoregulatory domain which is targeted by the inhibitor IPA-3, however the exact downstream inhibitory signalling pathway of IPA-3 is not clearly known yet. In addition, the role of CDC42 and Rho-GTPases in TNT formation is not fully investigated. A report of Hanna et al., (2017), demonstrated that the activity of CDC42 and Rho-GTPases positively contributes to the formation of TNTs in macrophages. In contrast, Delage et al., (2016); found that CDC42/IRSp53/VASP negatively regulates the formation of TNTs. On the other hand, oAβ is implicated in PAK1 dependent synaptic dysfunctions and PAK1 is aberrantly activated and translocated from the cytosol to the membrane during the development of pathology in the AD brain (Ma et al., 2008). Interestingly, HIV and HSV viruses exploit PAK1 kinase dependent macropinocytosis en route and recent studies have also shown direct cell-to-cell spreading of HIV and HSV virus via TNTs (Sowinski et al., 2008; Panasiuk et al., 2018). Interesting another report has shown that HIV-1 Nef protein mediated TNT formation associated with 5 proteins of exocyst complex and they involve in a PAK2 and Rab 11 dependent pathway (Mukerji et al., 2012). Additionally, alpha herpes virus induced TNT-like membrane actin projections depend on the conserved viral US3 serine/threonine protein kinase-dependent modulations of the cytoskeleton. These modulations are caused by activation of PAK1-dependent signalling and inhibition by IPA-3 clearly attenuates these TNT-like projections (Van Den Broeke et al., 2009; Jacob et al., 2015).

Several studies have suggested exosomes as a means of cell-to-cell transfer of Aβ (Rajendran *et al.*, 2006; Sardar Sinha *et al.*, 2018). However, such experiments were designed at non-physiological conditions using purified, concentrated exosomes from a large number of cultured cells. Additionally, a transfer mechanism via exosomes does not explain the

asymmetric spreading of oAβ microinjected in a single neuron of a primary hippocampal culture (Nath et al., 2012). Studies using the method of transwell assays have also shown the efficient cell-to-cell transfer of prion proteins despite the blocking of exosomes (Gousset *et al.*, 2009; Thayanithy *et al.*, 2017). These studies indicated a possible mechanism of direct cell-to-cell transfer via TNTs. On the other hand, organelles like toxic lysosomes have been demonstrated to propagate directly from cell-to-cell through TNTs (Victoria and Zurzolo, 2017). Here, we have clearly shown the direct cell-to-cell propagation of oAβ via TNTs. TNTs as a mean of direct neuron-to-neuron transfer is a convincing model of how oligomers that are suggested as initiator or driver of AD pathology could gradually progress through the anatomically connected brain regions. However, further in-depth studies are needed to understand how cells maintain homeostasis of intercellular communication by balancing exosome release and TNTs in the stressed cells.

The hypothesis is important in the context of progressive AD pathology development, as plaque pathology correlates poorly with progressive cognitive impairment in AD. Our study presented here shows that the sprouting of TNTs instigate the process of oAβ induced membrane damage and Ca^{++} dependent rapid membrane repair through lysosomal exocytosis via PAK1 dependent actin remodelling, probably to maintain cell surface area expansion and consequently membrane stress in equilibrium (Figure 8). It is very important to reveal the involvement of detailed molecular events of Pak1 dependent pinocytic vesicle recycling in relation to cell surface expansion and identification of upstream and downstream signaling of Pak1 dependent actin modulations, the pathways have been shown here to be involved in the induction of TNTs formation. The study presented here will open up a new avenue to unfold and explore an emerging novel pathway of intercellular cell-to-cell communication.

Material and Methods.

Preparation of soluble oAβ. Freshly made unlabelled oAβ and fluorescently labelled oAβ-TMR were prepared from lyophilized Aβ ($Aβ_{1–42}$) and Aβ-TMR ($Aβ_{1–42}$-5-tetramethyl rhodamin) suspended in 1,1,1,3,3,3-hexafluoro-2-propanol (AnaSpec). Lyophilized Aβ and Aβ-TMR were resuspended at a concentration of 5 mM in Me2SO and then diluted to a concentration of 100 μM in HEPES buffer, pH 7.4. The solution was immediately vortexed and sonicated for 2 min and then incubated at 4°C for 24 h (Catalano et al., 2006; Nath et al; Domert et al). Oligomers were characterized before the experiments similarly as reported in

our earlier papers (Nath *et al.*, 2012; Domert *et al.*, 2014), by electron microscopy imaging using a Jeol 1230 transmission electron microscope equipped with an ORIUS SC 1000 CCD camera, together with SDS-PAGE, Native-PAGE western blots and size exclusion chromatography.

Cell culture and differentiation of cells. SH-SY5Y neuronal cells (ECACC; Sigma-Aldrich) were seeded on 10-mm glass-bottom Petri dishes (MatTek) at a concentration of 12,000 cells/cm^2. Cells were partially differentiated with 10 µM retinoic acid (RA; Sigma-Aldrich) for 7 days. Pre-differentiated or partially differentiated SH-SY5Y cells were further differentiated for additional 10 days in 10-mm glass-bottom Petri dishes (MatTek) with brain-derived neurotrophic factor, neuregulin-1, nerve growth factor, and vitamin D3. After 10 days of differentiation on glass, the cells form long, branched neurites and several neurospecific markers, as described previously (Agholme *et al.*, 2010; Nath *et al.*, 2012). Partially differentiated and differentiated cells on glass petri dishes were incubated with 100–500 nM oAβ–TMR for 3 h at 37°C in a 5% CO_2 atmosphere. The cells were imaged after extensive PBS washing (two washes of 10 min each at 37°C with 5% CO_2). LysoTracker (green; Invitrogen) 50-250 nM was added 5-10 min before imaging.

oAβ internalization/uptake. To investigate the uptake mechanisms of Aβ in the used cell system, differentiated SH-SY5Y cells were pre-treated with inhibitors in growth medium for the indicated time and at the indicated concentration (Table 1). After washing with PBS, a final concentration of 0.5 µM oligomerised Aβ-TMR was added to the cells for 1.5 h. After removal of the reagents, the cells were kept in growth medium for 30 min before flow cytometry analysis. For flow cytometry, the cells were washed twice with PBS and trypsinised. The cells of 2 wells were resuspended in 300 µl PBS and filtered through a 50 µm nylon-mesh filter (Partec). The cells were analysed on a FACS Aria III flow cytometer (BD Biosciences) using FACSDiva acquisition software. Each treatment was carried out and analysed at least in triplicates. The gating was set using control cells without fluorophore and cells treated with Aβ-TMR only. The percentage of cells containing Aβ-TMR was calculated and normalised to the mean of Aβ-uptake without any inhibitor, resulting in a fold change, to make results from different experiments comparable. Kaluza Software (Beckman Coulter) was used for data analysis.

Table 1:

Pre-treatment conditions of used inhibitors for studying the mechanisms of oAβ uptake.

Inhibitor	Concentration	Treatment protocol
α-Bungaratoxin	100 nM	kept on at all time
AP-5 ((2R)-amino-5-phosphonopentanoate)	100 μM	kept on at all time
GYKI 52466 [4-(8-methyl-9H-1,3-dioxolo[4,5-h][2,3] benzodiazepin-5-yl)-benzenamine hydrochloride]	100 μM	kept on at all time
DPA (desipramine)	25 μM	2 h before experiment
Bafilomycin A1	10 nM	30 min before experiment
NH_4Cl	10 mM	30 min before experiment, no washing step, kept on at all time
MDC (monodansylcadaverine)	50 μM	30 min before experiment
PAO (phenylarsine oxide)	300 μM	30 min before experiment
Dynasore	80 μM	30 min before experiment
IPA-3 (1,1-Disulfanediyl-dinaphthalen-2-ol)	20 μM	30 min before experiment
EIPA (5-ethylisopropyl amiloride)	100 μM	30 min before experiment

Transformation of cells: For making competent cells, DH5α strain *E.coli* cells (3mL of overnight culture) were added to 50 mL of Luria-Bertani (LB) broth and incubated till the OD reached 0.6 to 0.8 at 600 nm. The culture was spun down at 3000 rpm and the pellet was treated with cold 0.15 M $CaCl_2$ in 15% glycerol solution. This step was continued two to three times, treating the pellet with $CaCl_2$ in order to make the cells competent.

For actin and membrane staining, two plasmids were used. The plasmid mEGFP-lifeact-7 (Addgene # 54610; Kanamycin resistant) was a gift from Michael Davidson and CAAX-mCherry (Ampicillin resistant) from Van Rheenen et al., 2007). The competent cells were removed from -80ºC and 1 µL of 1µg of each plasmid was added to it. Heat shock treatment was given for 90 seconds at 42ºC. The cells were placed in a bacterial incubator for an hour after heat shock and afterwards, were plated onto an LB agar plates containing 100 µg/mL of the appropriate antibiotic and left overnight for colonies to grow. The colonies that were able to grow on the plates were then isolated and allowed to grow in LB broth overnight. An 80% glycerol stock was made for the transformed bacterial cells to be used for isolation of the plasmids

Plasmid DNA purification: Plasmid DNA isolation was carried out using QIAGEN plasmid Midi kit. The plasmid purification protocols are based on a modified alkaline procedure followed by the binding of the plasmid DNA to QIAGEN resin under appropriate low-salt and pH-conditions. RNA, proteins, dyes and low-molecular-weight impurities are removed by a medium-salt wash. Plasmid DNA is eluted in a high-salt buffer and then concentrated and desalted by isopropanol precipitation.

Transfection of SH-SY5Y cells: Transfection of SH-SY5Y cells were done using jetPRIME transfection reagent (Polyplus). The cells were seeded in a 24 well plate in 0.5 mL culture media. The plasmid DNA (0.5 µg) was diluted in 50 µL of jetPRIME buffer and vortexed for 10 seconds. After this, 1.6 µL of jetPRIME reagent was added. The mixture was spun down and then incubated for 10 minutes at room temperature. The transcription mixture was then added to the cells in serum containing media and incubated between 24-48 hours.

Propidium Iodide staining: Undifferentiated SH-SY5Y cells were incubated with 1 µM of oAβ for 30 min or 1 h at 37 °C. Then the cells were washed and stained with propidium iodide (PI, 5 µg/ml) for 5 min. Cells were washed again two times with PBS before applying 4% PFA as fixative for 20 min at 4 °C. The fixed cells were observed by fluorescence microscopy or trypsinized before flow cytometry analysis.

Donor-acceptor 3D co-culture. Three dimensional donor-acceptor co-culturing was performed using RA treated partially differentiated cells for 10 days in ECM gel (1:1; Sigma-Aldrich), as described earlier (Nath *et al.*, 2012; Domert *et al.*, 2014). The differentiated cells in ECM gel have been well characterized previously; they had long, branched neurites, several neurospecific markers, synapse protein Sv2, axonal vesicle transport and mature splicing forms of tau (Agholme *et al.*, 2010; Nath *et al.*, 2012). The differentiated cells were stained green with EGFP-tagged (green) endosomal (Rab5a) or lysosomal (Lamp1) proteins using organelle lights BacMam-1.0 or 2.0 (Invitrogen). The green labelled differentiated cells were called 'acceptor cells'. Pre-differentiated cells (10 μM RA for 7 days in 35-mm cell-culture Petri dishes) incubated with 500 nM oAβ-TMR for 3 h at 37°C in a 5% CO_2 atmosphere; extensively washed using PBS (two washes of 10 min each at 37°C with 5% CO_2) and trypsinized, were denoted as 'donor cells' reseeded (40,000 cells per dish) on top of the acceptor cells after mixing (1:1) with pre-chilled ECM gel. Then, the 3D donor-acceptor co-cultured cells were incubated for 24 h with 10 μM RA at 37°C in a 5% CO_2 atmosphere.

Immunocytochemistry. Lamp1 staining on the luminal part of the PM in undifferentiated SH-SY5Y neuroblastoma cells was performed similarly as described earlier (Wäster et al., 2016), on unfixed cells. Cells were incubated for 15 and 30 min with 1 μM of oAβ in MEM media without FCS (fetal calf serum) supplement. Then, endocytosis of the cells was blocked with 5% BSA + 10% FCS in PBS for 5 min at 4 °C. Then cells were incubated with Lamp1-anti goat primary antibody (1:250, sc-8099, Santa Cruz Bio-technology; Santa Cruz, CA, USA; 2 h, 4 °C) in the blocking buffer for 45 min, followed by fixation of the cells in 4% PFA for 20 min at 4 °C before labelling with the secondary antigoat antibody conjugated to Alexa Fluor 488 (1:400 for 30 min; Molecular Probes, Eugene, OR, USA). Next, the cells were mounted in ProLong Gold antifade reagent supplemented with 4′,6-diamidino-2-phenylindole (DAPI; Molecular Probes).

Live cell imaging of membrane dynamics: oAβ (1 μM) was added concurrently with 1 μM of membrane binding dye TMA-DPH (N,N,N-Trimethyl-4-(6-phenyl-1,3,5-hexatrien-1-yl) phenylammonium p-toluenesulfonate; molecular formula: $C_{28}H_{31}NO_3S$) (10 mM of TMA-DPH stock solution was made by dissolving in methanol) and membrane dynamics of the live cells were followed by timelaps images using a confocal microscope. Excitation and emission maximum of TMA-DPH is 384 and 430 nm, with considerable tail of excitation spectra at 405

nm. Therefore, time-lapse images were taken using confocal-microscope by exciting the TMA-DPH dye using the 405 nm laser and sufficient emission light was collected using an opened pinhole. In this setup confocal microscope produces images similar to the widefield or epifluorescence images. Cultures were carried to the microscope one by one in 500 µl of 20 mM Hepes buffer of pH 7.4 maintaining the temperature at 37°C. oAβ (1 µM) was added concurrently with 1 µM of membrane binding dye TMA-DPH to HEK cells similarly as above and membrane dynamics of the live cells were studied by images taken by fluorescent microscope.

Confocal and fluorescence microscopy to image TNTs. Formation of oAβ induced TNTs were observed in the cells treated with incerasing concentrations of oAβ at different incubation times, using either confocal or fluorescence microscopes. The treatments were done by incubating the cells with oAβ in serum free medium and corresponding control cells were treated at the same conditions, to nullify the serum starvation induced TNTs. Images were acquired using a Zeiss LSM laser scanning confocal microscope using 63X/1.4 NA or 40X/1.3 NA oil immersion plan-apochromatic objective (Carl Zeiss AG, Oberkochen, Germany). The time-laps image sequences of the live cells were taken at 37°C by capturing simultaneously differential interference contrast (DIC) and fluorescence modes. Fluorescence microscopy (IX73-Olympus) with 40X/1.3 NA and 100X1.4 NA were also used to do the experiments of SH-SY5Y cells transfected with Plenti-lifeact EGFP plasmid and CAAX-mCherry plasmid. To study the effect of IPA-3 on SH-SY5Y cells, the cells were first treated with IPA-3 (20 mM) for 30 minutes followed by oAβ (1 µM) for 1 hour and 2 hours respectively. The cells were then visualized under fluorescence microscopy and numbers of TNTs were quantified by manual counting.

Flow-cytometry. Internalization of oAβ-TMR in presence and absence of inhibitors were quantified using BD FACS Aria ™ (BD Biosciences) and were analysed using BD FACS DIVA ™ (BD Bioscienc es) flow cytometer. Cells treated with propidium iodide (PI) were fixed, trypsinized and filtered using CellTrics 30 µm filters (Sysmex). Then re-suspended in PBS and quantified different sets either using BD FACS Aria ™ (BD Biosciences) or BD LSR II (BD Biosciences) flow cytometer and data were analysed using BD FACS DIVA ™ (BD Bioscienc es) flow cytometer.

Superresolution SIM images: All SIM (structured illumination microscopy) images were acquired using on DeltaVision OMX SR microscope from GE Healthcare using a 60X 1.42 NA objective and pco.edge sCMOS detector. The cells were fixed by 4% PFA by incubation for 15 min and fixed cells were imaged. The widefield images were deconvolved using the built-in algorithm.

Image analysis and statistics. Image analysis was done using ImageJ software (open source by NIH, USA). Percentage of co-localization of oAβ (red) with lysosomes (green) were performed by calculating the proportion of the red fluorescence pixels compared to the co-localized pixels from background subtracted images using Coloc-2 plugin. Cells with blebs / lamillopodia and TNTs were counted from images and normalized to the total number of cells. oAβ induced endocytosis was quantified by measuring the integrated intensities of internalized TMA-DPH from the luminal part of each cells by drawing ROI (region of interest) over sequences of time-laps confocal image stacks and comparing it with the same quantification of control cells. The fusion of lysosomal membrane to reseal the damaged membrane was detected as appearance of LAMP1 (green) on the outer leaflet of the PM. The outer leaflet LAMP1 was quantified measuring the integrated intensities from drawn ROI and proportionate percentage calculated comparing the total LAMP1 per cells. One-way ANOVA tests were performed to validate statistical significance in all experiments.

Acknowledgement: This research was made possible by funding of Assistant Professor intramural grants of Manipal Academy of Higher Education, India and Swedish Alzheimer's Foundation, Magnus Bergvalls and Gun och Bertil Stohnes research grants from Sweden. We thank our long-term collaborator Prof. Martin Hallbeck of Linkoping University, Sweden, for the valuable suggestions on designing of cell-to-cell transfer experiments. We thank Dr. Ravi Manjithaya of JNCASR, Bangalore, India, for giving us SH-SY5Y cell lines and giving access to the SIM-superresolution microscope. Thanks a lot to Likhesh Sharma, PhD, Product Manager GE Healthcare for assisting with imaging by SIM-superresolution microscope. We thank Prof. Satyajit Mayor of National centre for biological sciences, India, for his kind gift of sharing reagents and for his valuable inputs. CAAX-mCherry plasmid was obtained from Prof. Satyajit Mayor, which was a kind gift to Prof. Satyajit Mayor by Prof. Jacco van Rheenen of Hubrecht Institute for Developmental Biology and Stem Cell Research (KNAW). Thanks to Prof. Gopal Pande of Manipal institute of higher education, India, for reading the manuscript and for his valuable inputs.

Author Contributions: : S.N conceptualized and conducted the research; S.N and K.O designed research; S.N designed tunneling nanotube experiments; K.O. designed membrane dynamics and membrane repair experiments; N.D, A.D, C.K and S.N performed experiments; S.N, K.O and K.K interpreted data; S.N wrote the paper taking valuable inputs from all the authors.

References.

Abounit, S., J.W. Wu, K. Duff, G.S. Victoria, and C. Zurzolo. 2016. Tunneling nanotubes: A possible highway in the spreading of tau and other prion-like proteins in neurodegenerative diseases. *Prion*. 10:344–351.

Agholme, L., T. Lindström, K. Kgedal, J. Marcusson, and M. Hallbeck. 2010. An in vitro model for neuroscience: Differentiation of SH-SY5Y cells into cells with morphological and biochemical characteristics of mature neurons. *J. Alzheimer's Dis.* 20:1069–1082.

Andrews, N.W., and M. Corrotte. 2018. Plasma membrane repair. *Curr. Biol.*

Annunziata, I., A. Patterson, D. Helton, H. Hu, S. Moshiach, E. Gomero, R. Nixon, and A. D'Azzo. 2013. Lysosomal NEU1 deficiency affects amyloid precursor protein levels and amyloid-β secretion via deregulated lysosomal exocytosis. *Nat. Commun.* 4.

Apodaca, G. 2002. Modulation of membrane traffic by mechanical stimuli. *Am. J. Physiol. Renal Physiol.* 282:F179-90.

Appelqvist, H., P. Wäster, K. Kågedal, and K. Öllinger. 2013. The lysosome: From waste bag to potential therapeutic target. *J. Mol. Cell Biol.* 5:214–226.

Arispe, N., H.B. Pollard, and E. Rojas. 1993. Giant multilevel cation channels formed by Alzheimer disease amyloid beta-protein [A beta P-(1-40)] in bilayer membranes. *Proc. Natl. Acad. Sci. U. S. A.* 90:10573–7.

Bhat, S., C. Zurzolo, S. Zhu, S. Syan, Y. Kuchitsu, and M. Fukuda. 2018. Rab11a–Rab8a cascade regulates the formation of tunneling nanotubes through vesicle recycling. *J. Cell Sci.*

Bi, X., C.M. Gall, J. Zhou, and G. Lynch. 2002. Uptake and pathogenic effects of amyloid beta peptide 1-42 are enhanced by integrin antagonists and blocked by NMDA receptor antagonists. *Neuroscience*.

Van Den Broeke, C., M. Radu, M. Deruelle, H. Nauwynck, C. Hofmann, Z.M. Jaffer, J. Chernoff, and H.W. Favoreel. 2009. Alphaherpesvirus US3-mediated reorganization of the actin cytoskeleton is mediated by group A p21-activated kinases. *Proc. Natl. Acad. Sci. U. S. A.*

Bukoreshtliev, N. V., X. Wang, E. Hodneland, S. Gurke, J.F.V. Barroso, and H.H. Gerdes. 2009. Selective block of tunneling nanotube (TNT) formation inhibits intercellular organelle transfer between PC12 cells. *FEBS Lett.* 583:1481–1488.

Chen, D., C.R.M. Wilkinson, S. Watt, C.J. Penkett, W.M. Toone, N. Jones, and J. Bähler.

2008. Exocyst Requirement for Endocytic Traffic Directed Toward the Apical and Basolateral Poles of Polarized MDCK Cells. *Mol. Biol. Cell*.

Clavaguera, F., T. Bolmont, R.A. Crowther, D. Abramowski, S. Frank, A. Probst, G. Fraser, A.K. Stalder, M. Beibel, M. Staufenbiel, M. Jucker, M. Goedert, and M. Tolnay. 2009. Transmission and spreading of tauopathy in transgenic mouse brain. *Nat. Cell Biol.* 11:909–913.

Daniels, R.H., P.S. Hall, and G.M. Bokoch. 1998. Membrane targeting of p21-activated kinase 1 (PAK1) induces neurite outgrowth from PC12 cells. *EMBO J.*

Davis, D.M., and S. Sowinski. 2008. Membrane nanotubes: Dynamic long-distance connections between animal cells. *Nat. Rev. Mol. Cell Biol.* 9:431–436.

Deacon, S.W., A. Beeser, J.A. Fukui, U.E.E. Rennefahrt, C. Myers, J. Chernoff, and J.R. Peterson. 2008. An Isoform-Selective, Small-Molecule Inhibitor Targets the Autoregulatory Mechanism of p21-Activated Kinase. *Chem. Biol.*

Delage, E., D.C. Cervantes, E. Pénard, C. Schmitt, S. Syan, A. Disanza, G. Scita, and C. Zurzolo. 2016. Differential identity of Filopodia and Tunneling Nanotubes revealed by the opposite functions of actin regulatory complexes. *Sci. Rep.*

Desplats, P., H.-J. Lee, E.-J. Bae, C. Patrick, E. Rockenstein, L. Crews, B. Spencer, E. Masliah, and S.-J. Lee. 2009. Inclusion formation and neuronal cell death through neuron-to-neuron transmission of -synuclein. *Proc. Natl. Acad. Sci.* 106:13010–13015.

Dharmawardhane, S., A. Schurmann, M.A. Sells, J. Chernoff, S.L. Schmid, and G.M. Bokoch. 2000. Regulation of macropinocytosis by p21-activated kinase-1. *Mol. Biol. Cell*.

Dieriks, B.V., T.I.H. Park, C. Fourie, R.L.M. Faull, M. Dragunow, and M.A. Curtis. 2017. α-synuclein transfer through tunneling nanotubes occurs in SH-SY5Y cells and primary brain pericytes from Parkinson's disease patients. *Sci. Rep.* 7.

Ditaranto, K., T.L. Tekirian, and A.J. Yang. 2001. Lysosomal membrane damage in soluble Aβ-mediated cell death in Alzheimer's disease. *Neurobiol. Dis.* 8:19–31.

Domert, J., S.B. Rao, L. Agholme, A.C. Brorsson, J. Marcusson, M. Hallbeck, and S. Nath. 2014. Spreading of amyloid-β peptides via neuritic cell-to-cell transfer is dependent on insufficient cellular clearance. *Neurobiol. Dis.* 65:82–92.

Edgar, J.R., K. Willén, G.K. Gouras, and C.E. Futter. 2015. ESCRTs regulate amyloid precursor protein sorting in multivesicular bodies and intracellular amyloid-β accumulation. *J. Cell Sci.* 128:2520–2528.

Eriksson, I., S. Nath, P. Bornefall, A.M.V. Giraldo, and K. Öllinger. 2017. Impact of high cholesterol in a Parkinson's disease model: Prevention of lysosomal leakage versus stimulation of α-synuclein aggregation. *Eur. J. Cell Biol.* 96:99–109.

Freeman, D., R. Cedillos, S. Choyke, Z. Lukic, K. McGuire, S. Marvin, A.M. Burrage, S. Sudholt, A. Rana, C. O'Connor, C.M. Wiethoff, and E.M. Campbell. 2013. Alpha-Synuclein Induces Lysosomal Rupture and Cathepsin Dependent Reactive Oxygen Species Following Endocytosis. *PLoS One*. 8.

Gerdes, H.H., and R.N. Carvalho. 2008. Intercellular transfer mediated by tunneling nanotubes. *Curr. Opin. Cell Biol.* 20:470–475.

Gerdes, H.H., A. Rustom, and X. Wang. 2013. Tunneling nanotubes, an emerging intercellular communication route in development. *Mech. Dev.* 130:381–387.

Gibson, A.E., R.J. Noel, J.T. Herlihy, and W.F. Ward. 1989. Phenylarsine oxide inhibition of endocytosis: Effects on asialofetuin internalization. *Am. J. Physiol. - Cell Physiol.*

Gouras, G.K., D. Tampellini, R.H. Takahashi, and E. Capetillo-Zarate. 2010. Intraneuronal β-amyloid accumulation and synapse pathology in Alzheimer's disease. *Acta Neuropathol.* 119:523–541.

Gousset, K., E. Schiff, C. Langevin, Z. Marijanovic, A. Caputo, D.T. Browman, N. Chenouard, F. de Chaumont, A. Martino, J. Enninga, J.C. Olivo-Marin, D. Männel, and C. Zurzolo. 2009. Prions hijack tunnelling nanotubes for intercellular spread. *Nat. Cell Biol.* 11:328–336.

Gowrishankar, S., P. Yuan, Y. Wu, M. Schrag, S. Paradise, J. Grutzendler, P. De Camilli, and S.M. Ferguson. 2015. Massive accumulation of luminal protease-deficient axonal lysosomes at Alzheimer's disease amyloid plaques. *Proc. Natl. Acad. Sci.* 112:E3699–E3708.

Grant, B.D., and J.G. Donaldson. 2009. Pathways and mechanisms of endocytic recycling. *Nat. Rev. Mol. Cell Biol.*

Guo, S., X. Zhang, M. Zheng, X. Zhang, C. Min, Z. Wang, S.H. Cheon, M.H. Oak, S.Y. Nah, and K.M. Kim. 2015. Selectivity of commonly used inhibitors of clathrin-mediated and caveolae-dependent endocytosis of G protein-coupled receptors. *Biochim. Biophys. Acta - Biomembr.*

Hanna, S.J., K. McCoy-Simandle, V. Miskolci, P. Guo, M. Cammer, L. Hodgson, and D. Cox. 2017. The Role of Rho-GTPases and actin polymerization during Macrophage Tunneling Nanotube Biogenesis. *Sci. Rep.*

Hase, K., S. Kimura, H. Takatsu, M. Ohmae, S. Kawano, H. Kitamura, M. Ito, H. Watarai, C.C. Hazelett, C. Yeaman, and H. Ohno. 2009. M-Sec promotes membrane nanotube formation by interacting with Ral and the exocyst complex. *Nat. Cell Biol.* 11:1427–1432.

Idone, V., C. Tam, J.W. Goss, D. Toomre, M. Pypaert, and N.W. Andrews. 2008. Repair of injured plasma membrane by rapid Ca2+ dependent endocytosis. *J. Cell Biol.* 180:905–914.

Ilieva, H., M. Polymenidou, and D.W. Cleveland. 2009. Non-cell autonomous toxicity in neurodegenerative disorders: ALS and beyond. *J. Cell Biol.* 187:761–772.

Jacob, T., C. Van den Broeke, C. Van Waesberghe, L. Van Troys, and H.W. Favoreel. 2015. Pseudorabies virus US3 triggers RhoA phosphorylation to reorganize the actin cytoskeleton. *J. Gen. Virol.*

Julien, C., C. Tomberlin, C.M. Roberts, A. Akram, G.H. Stein, M.A. Silverman, and C.D. Link. 2018. In vivo induction of membrane damage by β-amyloid peptide oligomers. *Acta Neuropathol. Commun.* 6:131.

Kagan, B.L. 2012. Membrane pores in the pathogenesis of neurodegenerative disease. *Prog. Mol. Biol. Transl. Sci.* 107:295–325.

Kane, M.D., W.J. Lipinski, M.J. Callahan, F. Bian, R.A. Durham, R.D. Schwarz, A.E. Roher,

and L.C. Walker. 2000. Evidence for seeding of beta -amyloid by intracerebral infusion of Alzheimer brain extracts in beta -amyloid precursor protein-transgenic mice. *J. Neurosci.* 20:3606–11.

Kornhuber, J., M. Muehlbacher, S. Trapp, S. Pechmann, A. Friedl, M. Reichel, C. Mühle, L. Terfloth, T.W. Groemer, G.M. Spitzer, K.R. Liedl, E. Gulbins, and P. Tripal. 2011. Identification of novel functional inhibitors of acid sphingomyelinase. *PLoS One*.

LaFerla, F.M., K.N. Green, and S. Oddo. 2007. Intracellular amyloid-beta in Alzheimer's disease. *Nat. Rev. Neurosci.* 8:499–509.

Li, Y., D. Cheng, R. Cheng, X. Zhu, T. Wan, J. Liu, and R. Zhang. 2014. Mechanisms of U87 astrocytoma cell uptake and trafficking of monomeric versus protofibril Alzheimer's disease amyloid-β proteins. *PLoS One*.

Loh, J., M.C. Chuang, S.S. Lin, J. Joseph, Y.A. Su, T.L. Hsieh, Y.C. Chang, A.P. Liu, and Y.W. Liu. 2019. An acute decrease in plasma membrane tension induces macropinocytosis via PLD2 activation. *J. Cell Sci.*

Ma, Q.L., F. Yang, F. Calon, O.J. Ubeda, J.E. Hansen, R.H. Weisbart, W. Beech, S.A. Frautschy, and G.M. Cole. 2008. p21-activated kinase-aberrant activation and translocation in Alzheimer disease pathogenesis. *J. Biol. Chem.*

Macia, E., M. Ehrlich, R. Massol, E. Boucrot, C. Brunner, and T. Kirchhausen. 2006. Dynasore, a Cell-Permeable Inhibitor of Dynamin. *Dev. Cell*.

Mandrekar, S., Q. Jiang, C.Y.D. Lee, J. Koenigsknecht-Talboo, D.M. Holtzman, and G.E. Landreth. 2009. Microglia mediate the clearance of soluble aβ through fluid phase macropinocytosis. *J. Neurosci.*

McLaurin, J., and A.Y. Lai. 2011. Mechanisms of amyloid-beta peptide uptake by neurons: The role of lipid rafts and lipid raft-associated proteins. *Int. J. Alzheimers. Dis.*

Melki, R., J.-Y. Li, E. Angot, C. Hansen, P. Brundin, J.A. Steiner, T.F. Outeiro, A.-L. Bergström, P. Kallunki, G. Paul, K. Fog, and L. Pieri. 2011. α-Synuclein propagates from mouse brain to grafted dopaminergic neurons and seeds aggregation in cultured human cells. *J. Clin. Invest.* 121:715–725.

Mercer, J., and A. Helenius. 2009. Virus entry by macropinocytosis. *Nat. Cell Biol.*

Meyer-Luehmann, M., J. Coomaraswamy, T. Bolmont, S. Kaeser, C. Schaefer, E. Kilger, A. Neuenschwander, D. Abramowski, P. Frey, A.L. Jaton, J.M. Vigouret, P. Paganetti, D.M. Walsh, P.M. Mathews, J. Ghiso, M. Staufenbiel, L.C. Walker, and M. Jucker. 2006. Exogenous induction of cerebral β-amyloidogenesis is governed bf agent and host. *Science (80-.).* 313:1781–1784.

Mukerji, J., K.C. Olivieri, V. Misra, K.A. Agopian, and D. Gabuzda. 2012. Proteomic analysis of HIV-1 Nef cellular binding partners reveals a role for exocyst complex proteins in mediating enhancement of intercellular nanotube formation. *Retrovirology*.

Narasimhan, S., J.L. Guo, L. Changolkar, A. Stieber, J.D. McBride, L. V. Silva, Z. He, B. Zhang, R.J. Gathagan, J.Q. Trojanowski, and V.M.Y. Lee. 2017. Pathological Tau Strains from Human Brains Recapitulate the Diversity of Tauopathies in Nontransgenic Mouse Brain. *J. Neurosci.* 37:11406–11423.

Nath, S., L. Agholme, F.R. Kurudenkandy, B. Granseth, J. Marcusson, and M. Hallbeck.

2012. Spreading of neurodegenerative pathology via neuron-to-neuron transmission of β-amyloid. *J. Neurosci.* 32.

Onfelt, B., S. Nedvetzki, K. Yanagi, and D.M. Davis. 2004. Cutting edge: Membrane nanotubes connect immune cells. *J. Immunol.* 173:1511–3.

Panasiuk, M., M. Rychłowski, N. Derewońko, and K. Bieńkowska-Szewczyk. 2018. Tunneling Nanotubes as a Novel Route of Cell-to-Cell Spread of Herpesviruses. *J. Virol.* 92.

Poëa-Guyon, S., M.R. Ammar, M. Erard, M. Amar, A.W. Moreau, P. Fossier, V. Gleize, N. Vitale, and N. Morel. 2013. The V-ATPase membrane domain is a sensor of granular ph that controls the exocytotic machinery. *J. Cell Biol.*

Prusiner, S.B. 2013. Biology and Genetics of Prions Causing Neurodegeneration. *Annu. Rev. Genet.* 47:601–623.

Rajendran, L., M. Honsho, T.R. Zahn, P. Keller, K.D. Geiger, P. Verkade, and K. Simons. 2006. Alzheimer's disease beta-amyloid peptides are released in association with exosomes. *Proc. Natl. Acad. Sci.* 103:11172–11177.

Ren, P.H., J.E. Lauckner, I. Kachirskaia, J.E. Heuser, R. Melki, and R.R. Kopito. 2009. Cytoplasmic penetration and persistent infection of mammalian cells by polyglutamine aggregates. *Nat. Cell Biol.* 11:219–225.

Van Rheenen, J., X. Song, W. Van Roosmalen, M. Cammer, X. Chen, V. DesMarais, S.C. Yip, J.M. Backer, R.J. Eddy, and J.S. Condeelis. 2007. EGF-induced PIP2 hydrolysis releases and activates cofilin locally in carcinoma cells. *J. Cell Biol.*

Rustom, A. 2016. The missing link: Does tunnelling nanotube-based supercellularity provide a new understanding of chronic and lifestyle diseases? *Open Biol.* 6.

Rustom, A., R. Saffrich, I. Markovic, P. Walther, and H.H. Gerdes. 2004. Nanotubular Highways for Intercellular Organelle Transport. *Science (80-.).* 303:1007–1010.

Sannerud, R., C. Esselens, P. Ejsmont, R. Mattera, L. Rochin, A.K. Tharkeshwar, G. De Baets, V. De Wever, R. Habets, V. Baert, W. Vermeire, C. Michiels, A.J. Groot, R. Wouters, K. Dillen, K. Vints, P. Baatsen, S. Munck, R. Derua, E. Waelkens, G.S. Basi, M. Mercken, M. Vooijs, M. Bollen, J. Schymkowitz, F. Rousseau, J.S. Bonifacino, G. Van Niel, B. De Strooper, and W. Annaert. 2016. Restricted Location of PSEN2/γ-Secretase Determines Substrate Specificity and Generates an Intracellular Aβ Pool. *Cell.* 166:193–208.

Sardar Sinha, M., A. Ansell-Schultz, L. Civitelli, C. Hildesjö, M. Larsson, L. Lannfelt, M. Ingelsson, and M. Hallbeck. 2018. Alzheimer's disease pathology propagation by exosomes containing toxic amyloid-beta oligomers. *Acta Neuropathol.* 136:41–56.

Sartori-Rupp, A., D. Cordero Cervantes, A. Pepe, K. Gousset, E. Delage, S. Corroyer-Dulmont, C. Schmitt, J. Krijnse-Locker, and C. Zurzolo. 2019. Correlative cryo-electron microscopy reveals the structure of TNTs in neuronal cells. *Nat. Commun.*

Sells, M.A., J.T. Boyd, and J. Chernoff. 1999. p21-Activated kinase 1 (Pak1) regulates cell motility in mammalian fibroblasts. *J. Cell Biol.*

Sowinski, S., C. Jolly, O. Berninghausen, M.A. Purbhoo, A. Chauveau, K. Köhler, S. Oddos, P. Eissmann, F.M. Brodsky, C. Hopkins, B. Önfelt, Q. Sattentau, and D.M. Davis. 2008.

Membrane nanotubes physically connect T cells over long distances presenting a novel route for HIV-1 transmission. *Nat. Cell Biol.* 10:211–219.

Tardivel, M., S. Bégard, L. Bousset, S. Dujardin, A. Coens, R. Melki, L. Buée, and M. Colin. 2016. Tunneling nanotube (TNT)-mediated neuron-to neuron transfer of pathological Tau protein assemblies. *Acta Neuropathol. Commun.* 4:117.

Thayanithy, V., P. O'Hare, P. Wong, X. Zhao, C.J. Steer, S. Subramanian, and E. Lou. 2017. A transwell assay that excludes exosomes for assessment of tunneling nanotube-mediated intercellular communication. *Cell Commun. Signal.* 15:1–16.

Thottacherry, J.J., A.J. Kosmalska, A. Kumar, A.S. Vishen, A. Elosegui-Artola, S. Pradhan, S. Sharma, P.P. Singh, M.C. Guadamillas, N. Chaudhary, R. Vishwakarma, X. Trepat, M.A. del Pozo, R.G. Parton, M. Rao, P. Pullarkat, P. Roca-Cusachs, and S. Mayor. 2018. Mechanochemical feedback control of dynamin independent endocytosis modulates membrane tension in adherent cells. *Nat. Commun.* 9.

Venkitaramani, D. V., J. Chin, W.J. Netzer, G.K. Gouras, S. Lesne, R. Malinow, and P.J. Lombroso. 2007. -Amyloid Modulation of Synaptic Transmission and Plasticity. *J. Neurosci.* 27:11832–11837.

Victoria, G.S., and C. Zurzolo. 2017. The spread of prion-like proteins by lysosomes and tunneling nanotubes: Implications for neurodegenerative diseases. *J. Cell Biol.* 216:2633–2644.

Walsh, D.M., and D.J. Selkoe. 2004. Deciphering the molecular basis of memory failure in Alzheimer's disease. *Neuron*. 44:181–93.

Wang, Y., J. Cui, X. Sun, and Y. Zhang. 2011. Tunneling-nanotube development in astrocytes depends on p53 activation. *Cell Death Differ.* 18:732–742.

Wäster, P., I. Eriksson, L. Vainikka, I. Rosdahl, and K. Öllinger. 2016. Extracellular vesicles are transferred from melanocytes to keratinocytes after UVA irradiation. *Sci. Rep.* 6.

Wei, W., L.N. Nguyen, H.W. Kessels, H. Hagiwara, S. Sisodia, and R. Malinow. 2010. Amyloid beta from axons and dendrites reduces local spine number and plasticity. *Nat. Neurosci.* 13:190–196.

Xie, H.R., L. Sen Hu, and G.Y. Li. 2010. SH-SY5Y human neuroblastoma cell line: In vitro cell model of dopaminergic neurons in Parkinson's disease. *Chin. Med. J. (Engl).*

Yang, W.N., K.G. Ma, X.L. Chen, L.L. Shi, G. Bu, X.D. Hu, H. Han, Y. Liu, and Y.H. Qian. 2014. Mitogen-activated protein kinase signaling pathways are involved in regulating α7 nicotinic acetylcholine receptor-mediated amyloid-β uptake in SH-SY5Y cells. *Neuroscience*.

Zhao, W.Q., F. Santini, R. Breese, D. Ross, X.D. Zhang, D.J. Stone, M. Ferrer, M. Townsend, A.L. Wolfe, M.A. Seager, G.G. Kinney, P.J. Shughrue, and W.J. Ray. 2010. Inhibition of calcineurin-mediated endocytosis and α-amino-3-hydroxy- 5-methyl-4-isoxazolepropionic acid (AMPA) receptors prevents amyloid β oligomer-induced synaptic disruption. *J. Biol. Chem.*

Zhu, S., G.S. Victoria, L. Marzo, R. Ghosh, and C. Zurzolo. 2015. Prion aggregates transfer through tunneling nanotubes in endocytic vesicles. *Prion*. 9:125–135.

Figure Legends:

Figure 1: Formation of TNTs is independent of differentiation stages of neuronal cells. A) SH-SY5Y cells incubated with extracellularly applied oAβ (1 μM) internalize efficiently to early-endosomes (Rab 5) and late-endosomes (MVB) or lysosomes (Lamp1) in substantial quantity. The images shown here were taken after 1.5 h of incubation. B) Connected nanotubes (highlighted by rectangle boxes) between neighbouring cells detected in differentiated SH-SY5Y cells incubated for 3 h with 500 nM of oAβ-TMR (red), washed and stained with 50 nM of lysotracker (green) before capture of the image. The cells with long TNTs form noticeable blebs, filopodium and cell membrane expansion (indicated by black arrows). C) Differentiated control cells show neuritic connections. Note that the cells are also devoid of TNTs and unusual blebs or filopodium like structures. D) Percentages of cells with blebs / lamellipodia were quantified from the images taken with increasing concentrations of oAβ-TMR (200-500 nM) and compared with the control cells. E) Similarly, TNTs were quantified with respect to the total number of cells. F-G) Partially differentiated SH-SY5Y cells were incubated with 250 nM of oAβ-TMR (red) for 3 h, washed and labelled with 200 nM of lysotracker (green). Cells internalized oAβ-TMR and eventually accumulate to MVB/lysosomes. F) oAβ-TMR internalized cell makes network between 3 neighbouring cells via formation of TNTs (white arrows), extended from lamellipodia-like membrane protrusions (black arrows). G) TNTs form networks between two neighbouring cells. H) Partially differentiated control cells devoid of blebs / lamellipodia. I) Percentages of cells with blebs / lamellipodia in oAβ-TMR treated cells were quantified and compared with the control cells. Number of TNTs were quantified by manually counting from cell images and plotted with respect to the total number of cells in percentage. Quantifications were done from > 60 cells in each set. n > 3. Plots are mean ± SD. One-way ANOVA tests were performed to validate statistical significance. Scale bars are 10 μm.

Figure 2: TNTs propagate oAβ and organelles from one cell to another. A) Partially differentiated SH-SY5Y cells were incubated with 250 nM of oAβ-TMR (red) for 3 h, washed and labelled with 200 nM of lysotracker (green). A) The cells form thin TNTs extended from expanded lamellipodia-like membrane protrusions (black arrows). oAβ-TMR co-localized with

lysosomes moves from one cell to another via connected tube (white arrows). B) Differentiated SH-SY5Y cells were incubated with 500 nM of oAβ-TMR (red) for 3 h, washed and labelled with 50 nM of lysotracker (green). The cells form TNTs and oAβ-TMR travels from one cell-to-another as organelles like puncta structures through the TNT (white arrows). A sequence of images at different time points is presented. C) Differentiated control cells form numerous networks of neurites, stained with early endosomal marker Rab5 (green) and mitotracker (red) in a merged image. Middle and right image show differentiated cells after 6 h incubation with oAβ (500 nm) with TNT-like thin connections direct from one cell-to-another, with early endosomal marker rab5 (green) and mitotracker (red) labelled organelles. However, neurites are degraded by oAβ incubation in a time and concentration dependent manner (Supplementary Figure 1). Scale bars are 10 μm.

Figure 3: oAβ induced PM damage and repair via coupled lysosomal-exocytosis and endocytosis. A) Undifferentiated SH-SY5Y cells were incubated with and without 1 μM of oAβ together with the membrane dye TMA-DPH (0.5 μM) and imaged immediately after addition. Formation of TNTs (white arrows) was observed in the cells with 1 μM of oAβ (images are after 2 and 15 min), preceding of massive membrane activities, filopodium formation and endocytosis of membranes. Control cells (without oAβ) show no filopodium, TNTs or massive membrane activities. B) Internalization or endocytosis of PM labelled with TMA-DPH was quantified in control and oAβ-treated cells by measuring luminal part intensities over time. The plot is mean intensities with SD (quantified > 20 cells from each set, n = 3). C) In oAβ (1h with 1 μM) treated cells, there is change in membrane fluidity, which causes the penetration of the membrane impermeable dye TMA-DPH. However, cells show no cell death when tested with the MTT or XTT assays (Supplementary Figure 1), but appear with relatively stable TNTs. E) Enhanced Lamp1 surface staining was detected in undifferentiated SH-SY5Y cells within 30 min of exposure of oAβ (1 μM), as an indicator of lysosomal membrane fusion with the PM as mechanism of membrane repair processes. F) Lamp1 surface staining was quantified from intensity (plotted mean ± SD) measurements by defined ROI using ImageJ. (n=3, each dot represents the number of cells). F) oAβ (1 μM) induced membrane damage in undifferentiated SH-SY5Y cells, detected as uptake of the membrane-impermeable dye propidium iodide (PI) in presence and absence of 5 mM EGTA (without Ca^{++}) in PBS. Significant enhancement of PI uptake within 1 h after oAβ treatment was observed and quantified by flow cytometry (n = 6). G) Penetration of PI was quantified using flow cytometer

and presented as change of median fluorescence in control and oAβ treated cells in presence and absence of Ca^2 in buffer. H) Representative confocal images. One-way ANOVA tests were performed to validate statistical significance. Scale bars are 5 μm.

Figure 4. Mechanisms of rapid internalization of oAβ-TMR was identified by pre-treating the partially differentiated SH-SY5Y cells with different endocytosis and receptor inhibitors. The percentage of oAβ-TMR containing cells was analysed by flow cytometry. A) Cells were pretreated with the receptor inhibitors α-Bunga, AP-5, GYKI. n=1, triplicates. B) Cells were pretreated with endocytosis inhibitors Dyna, DPA, MDC, PAO, NH4Cl, Baf, IPA-3 and EIPA, followed by exposure to 0.5 μm oAβ-TMR for 1h. n= 3, > minimum of duplicates in each sets. The percentage values were normalized to the respective mean of oAβ. C) Representative dot-plots with forward scatter vs fluorescence intensities (TMR). D) Representative confocal images with endocytosis inhibitors in undifferentiated SH-SY5Y cells. One-way ANOVA tests were performed to validate statistical significance. Scale bar = 10 μm.

Figure 5. Inhibition of rapid internalization of oAβ by the PAK 1 inhibitor IPA-3 can also inhibit formation of TNTs. A) Fluorescence microscopy images were taken using undifferentiated SH-SY5Y cells transfected with lifeact EGFP plasmid to stain f-actin. Upper images show control cells and cells treated with oAβ (1 h) with TNTs marked with arrows. Lower images show IPA-3 treated and cells treated with IPA-3 and then oAβ. B) Cells were also stained with CAAX-mCherry to stain a peripheral membrane protein. The co-transfected cells showed TNTs are co-stained with actin and peripheral membrane protein CAAX. C) Number of TNTs were counted to quantify the inhibition by IPA-3. n=3 and number of cells > 30 for each set. Plotted mean ± SD. One-way ANOVA tests were performed to validate statistical significance. Scale bar = 10 μm.

Figure 6. Super-resolution SIM images reveal that PAK1 inhibitor IPA-3 inhibits TNTs by remodulating f-actin. Super resolution images of lifeact stained SH-SY5Y cells by DeltaVision™ OMX SR microscopy. SH-SY5Y cells were transfected with Plenti-lifeact EGFP plasmid and treated with oAβ (1μM) and IPA-3 (20μM). A) In oAβ (1 h) treated cells, TNTs appear to spread out as extensions from the long f-actin of the cytoskeleton and to connect the two neighbouring cells. $A^{/}$) Zoomed image of a proper z-stack illustrates clearly the f-actin labelled connected TNT between neighbouring cells. $A^{//}$) 3D volume view of z-stacks of SIM image shows that, in contrast to neurons, TNTs do not touch the substratum, but rather stay "hung" between the two connected cells even after the fixation of the cells. B) In oAβ (1 h) treated cells, numerous long f-actins were noticed and they also formed bunches of long fibres. C) In the oAβ+ IPA-3 treated cells, disruptions of long stretched f-actins

of cytoskeleton and inhibition of TNTs are present. 3D reconstructions and analysis were done using ImageJ. Scale bar = 10 μm.

Figure 7. Accumulated endogenous oAβ with transferred oligomers from donor cells can also induce TNTs. The 3D donor-acceptor cell model was designed to allow donor cells to accumulate oAβ-TMR (red) before they were co-cultured for 24 h with acceptor cells transfected with EGFP-tagged (green) Rab 5. A) Part of the image has already been demonstrated in (Nath et al., 2012) to show cell-to-cell transfer between donor to acceptor cell. Here we have shown that TNT formed towards a healthy acceptor cell (marked 2) from the acceptor cell (marked 1) that already accumulated oAβ-TMR. Box 1 shows induction of transient filopodium (black arrows) from acceptor cell-1, that already accumulated with oAβ-TMR. Box 2 shows TNT formation from expanded membrane protrusions (white arrow) from the stressed acceptor cell to healthy one. Healthy acceptor cell (marked 2) received very little amount of oAβ-TMR (yellow arrow) form the stressed acceptor cell (marked 2). B) The transferred non-degradable oAβ-TMR (red) ends up to MVB/lysosomes (Lamp 1, green) of acceptor cells in the co-cultured cells and often was observed co-localised with TNTs between two acceptor cells. The gradual accumulation of oligomers in acceptor cells causes formation of extra-large MVB/lysosomes after 48 h. C) Percentage of cells with blebs / lamellipodia in oAβ-TMR accumulated donor and acceptor cells was quantified by counting images after 24 h of co-culture and compared with the healthy acceptor cells with no accumulation of oAβ-TMR. D) Number of TNTs was also quantified with respect to the total number of donor and acceptor cells, respectively. Quantifications were done from > 30 cells in each set. Plots are mean ± SD. One-way ANOVA tests were performed to validate statistical significance. Scale bar is10 μm.

Figure 8. Schematic summary to show that the sprouting of TNTs instigate in the process of oAβ induced membrane damage and rapid membrane repair process via PAK1 kinase dependent recycling of pinocytic vesicles and actin remodeling. The cartoon shows oAβ (red circles) induced PM damage and repair via coupled lysosomal-exocytosis and endocytosis to re-establish the PM. TNTs transfer oligomers directly from one cell-to-another.

Figures

Figure 1

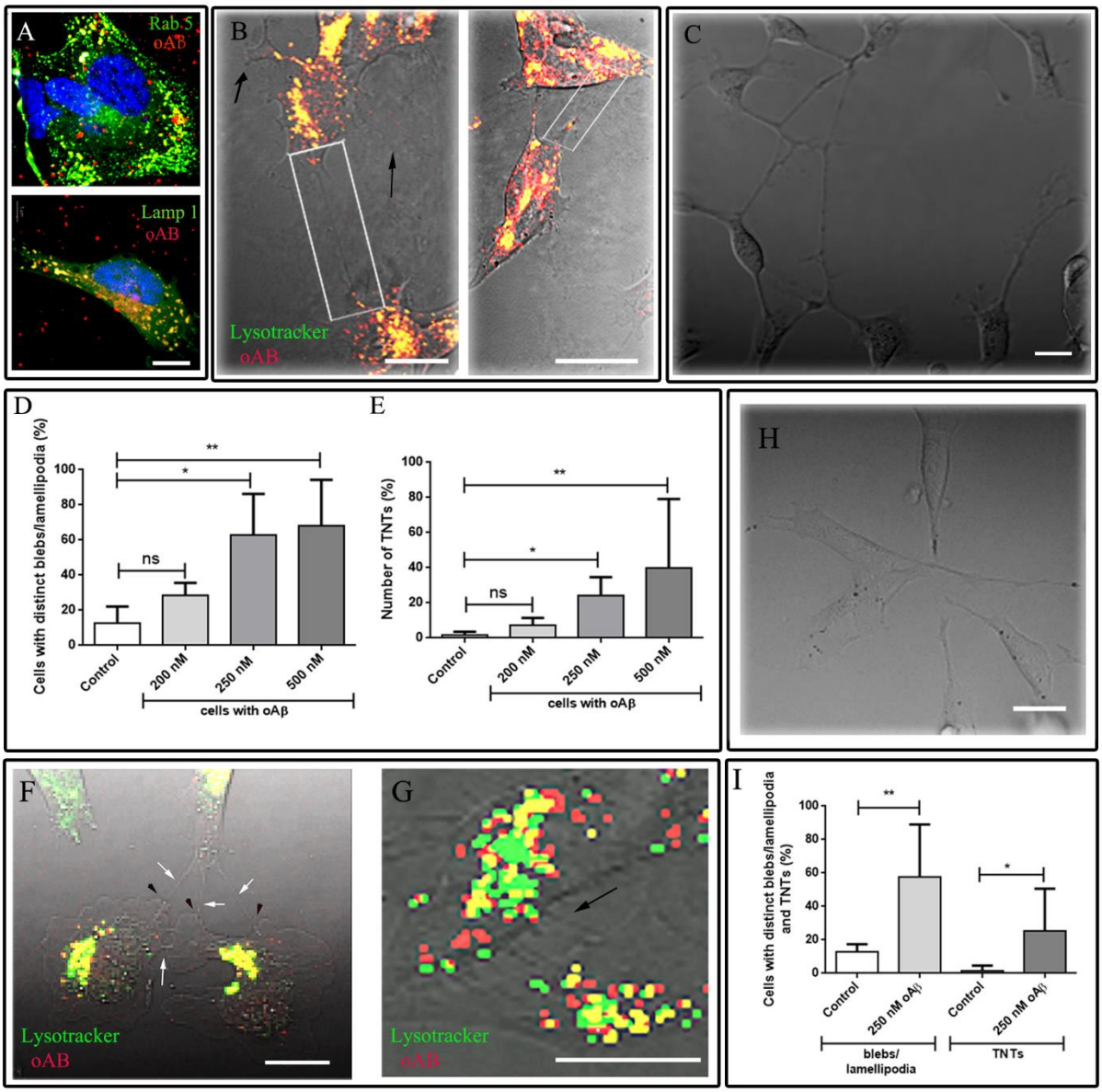

Figure 2

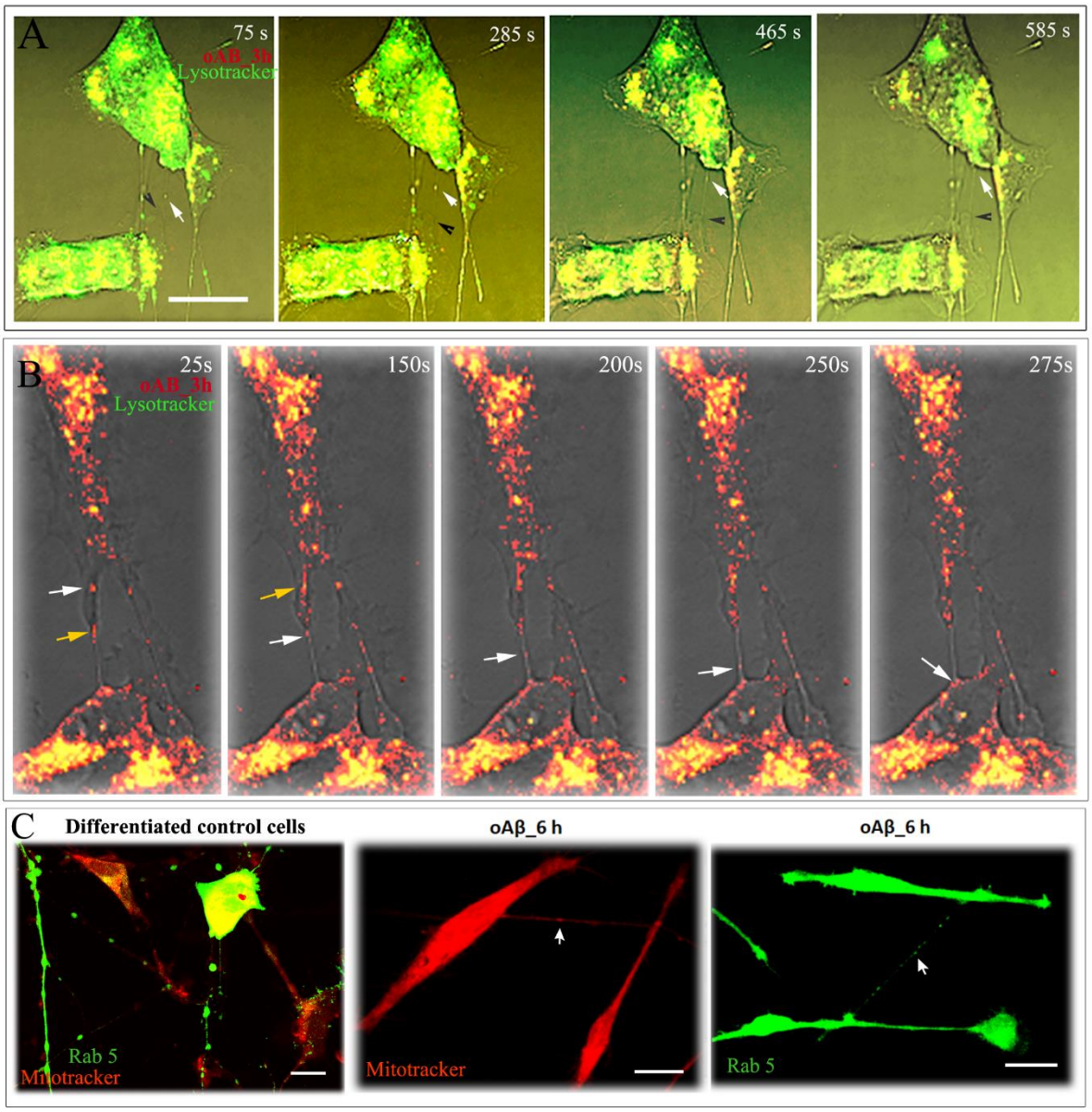
A
75 s
oAB_3h
Lysotracker
285 s
465 s
585 s
B
25s
oAB_3h
Lysotracker
150s
200s
250s
275s
C
Differentiated control cells
oAβ_6 h
oAβ_6 h
Rab 5
Mitotracker
Mitotracker
Rab 5

Figure 3

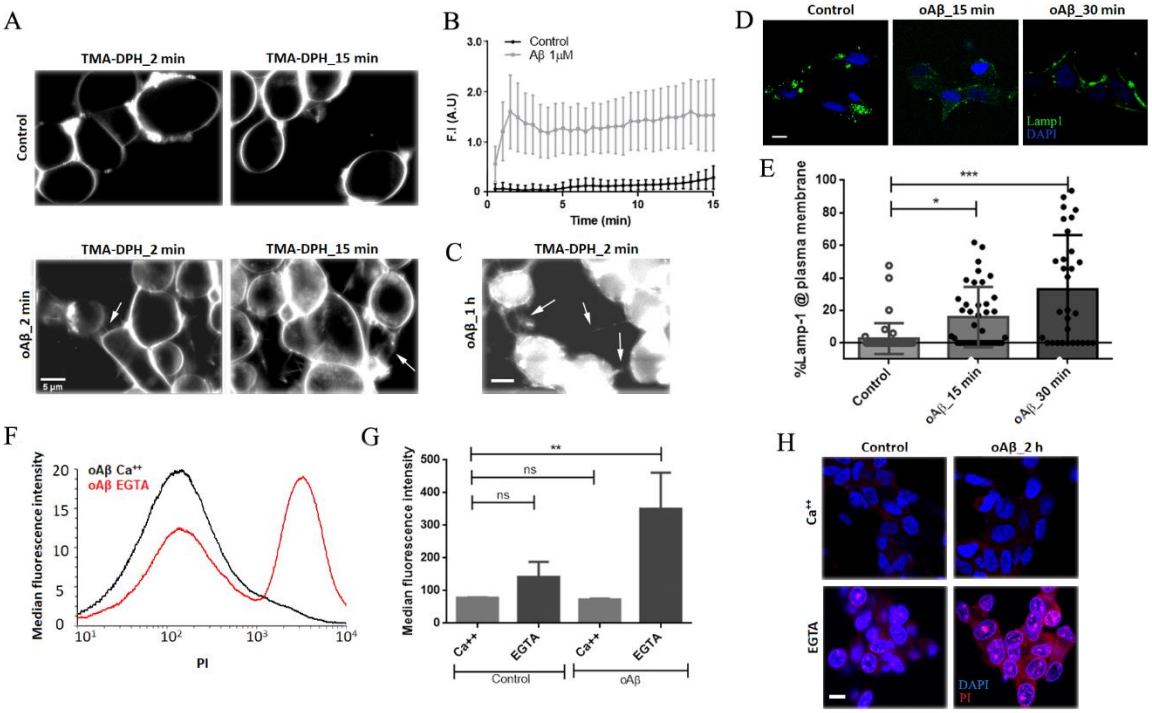
A
TMA-DPH_2 min
TMA-DPH_15 min
Control
oAβ_2 min
5 µm
B
Control
Aβ 1µM
F.I (A.U)
Time (min)
C
TMA-DPH_2 min
oAβ_1 h
D
Control
oAβ_15 min
oAβ_30 min
Lamp1
DAPI
E
%Lamp-1 @ plasma membrane
Control
oAβ_15 min
oAβ_30 min
F
oAβ Ca++
oAβ EGTA
Median fluorescence intensity
PI
G
Median fluorescence intensity
ns
ns
**
Ca++
EGTA
Ca++
EGTA
Control
oAβ
H
Control
oAβ_2 h
Ca++
EGTA
DAPI
PI

Figure 4

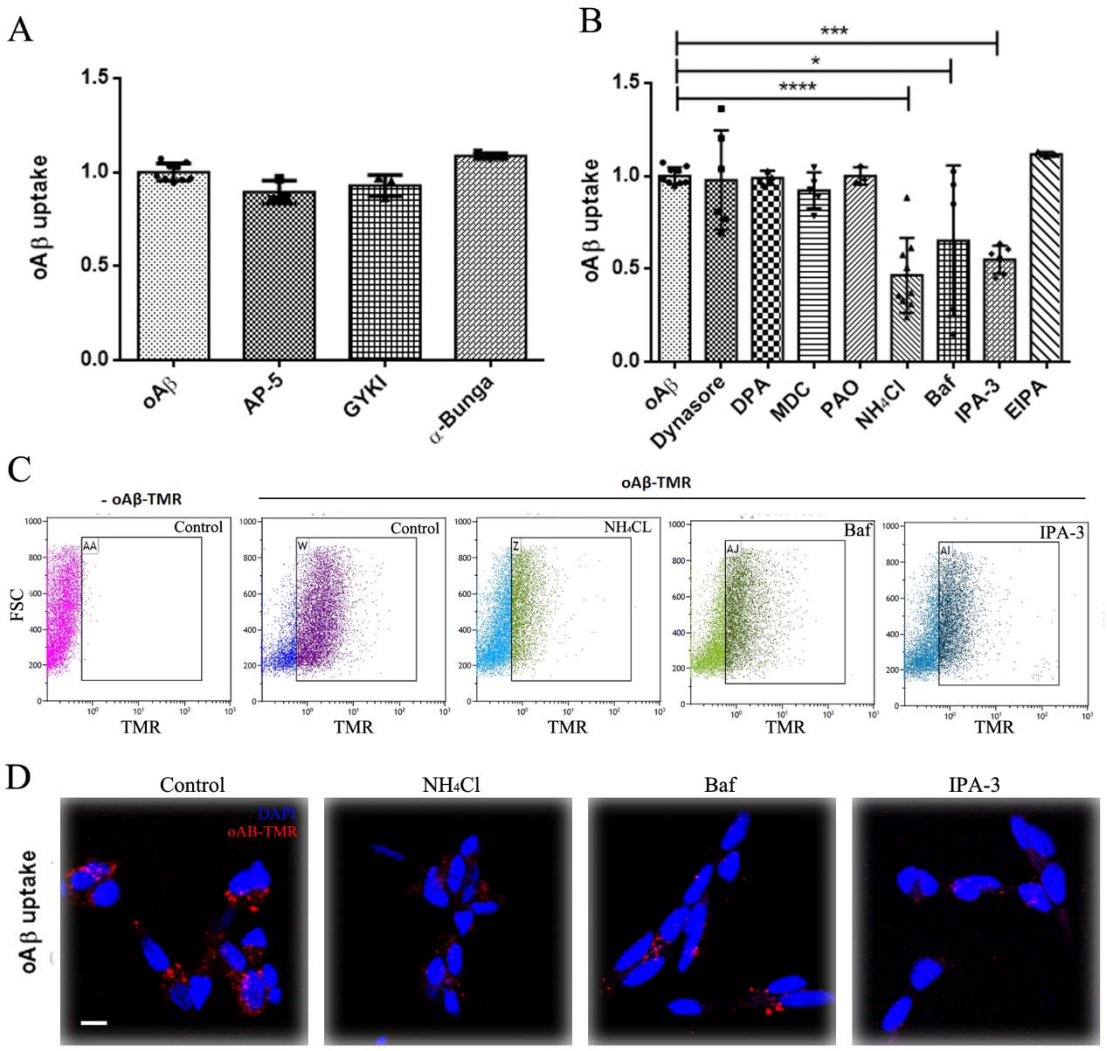
A
oAβ uptake
1.5
1.0
0.5
0.0
oAβ
AP-5
GYKI
α-Bunga
B
***
*
****
oAβ uptake
oAβ
Dynasore
DPA
MDC
PAO
NH4Cl
Baf
IPA-3
EIPA
C
- oAβ-TMR
oAβ-TMR
Control
NH4CL
Baf
IPA-3
FSC
TMR
D
Control
NH4Cl
Baf
IPA-3
DAPI
oAB-TMR
oAβ uptake

Figure 5

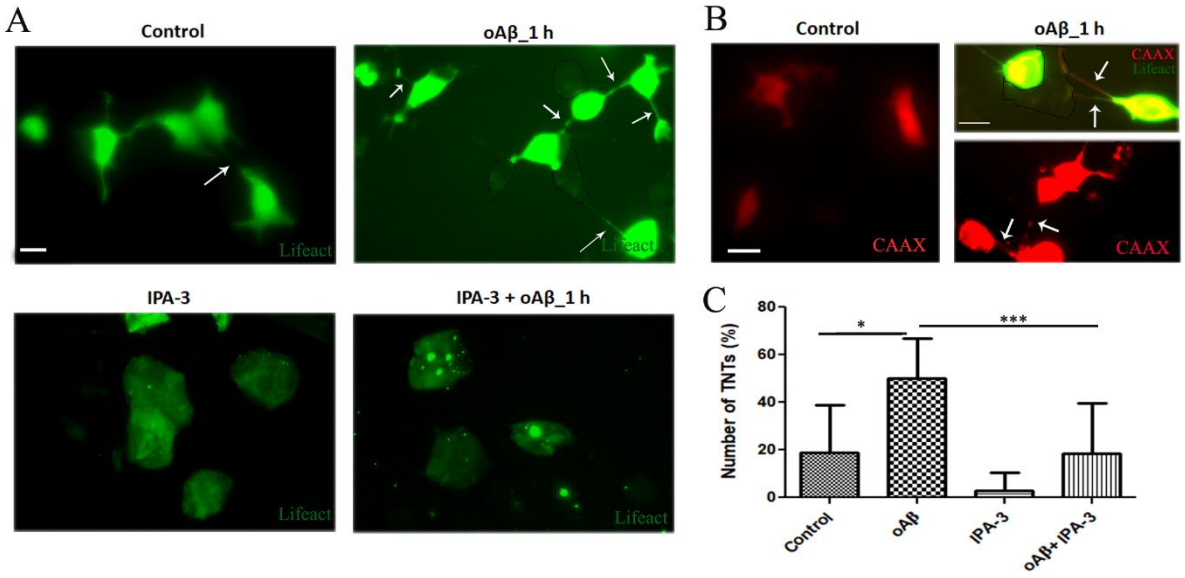
A
Control
oAβ_1 h
IPA-3
IPA-3 + oAβ_1 h
Lifeact
B
Control
oAβ_1 h
CAAX
Lifeact
C
Number of TNTs (%)
80
60
40
20
0
*
***
Control
oAβ
IPA-3
oAβ+ IPA-3

Figure 6

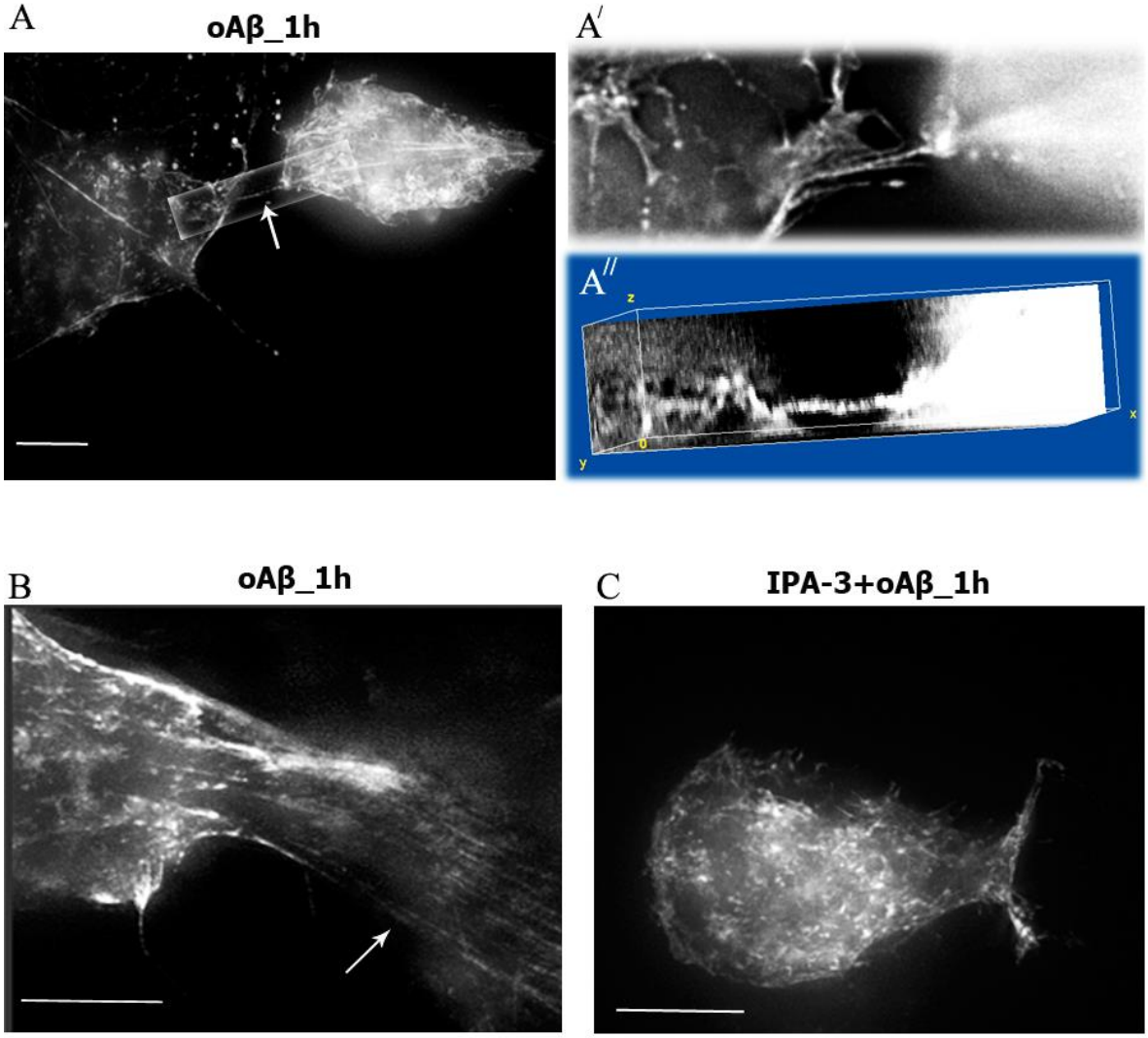

Figure 7

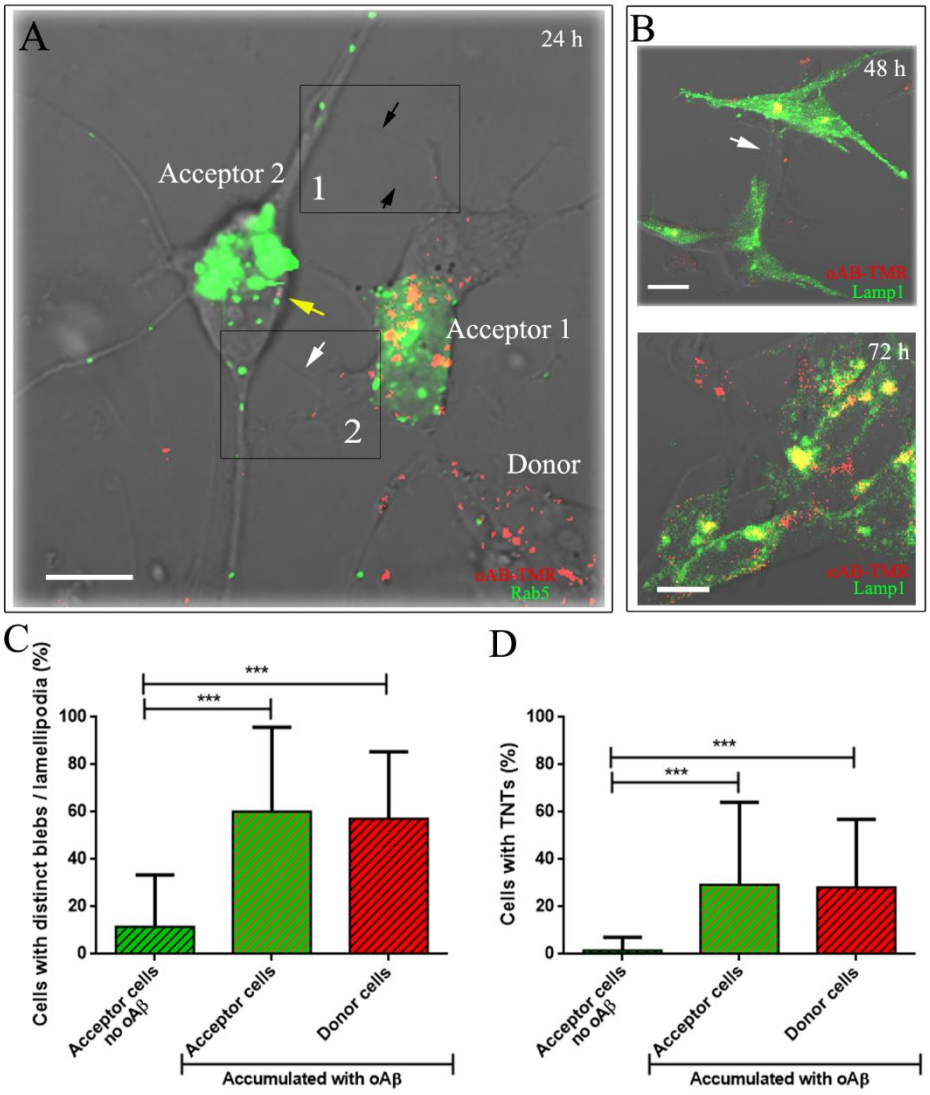
A
24 h
Acceptor 2
1
Acceptor 1
2
Donor
oAβ-TMR
Rab5
B
48 h
oAβ-TMR
Lamp1
72 h
oAβ-TMR
Lamp1
C
Cells with distinct blebs / lamellipodia (%)
***
***
100
80
60
40
20
0
Acceptor cells no oAβ
Acceptor cells
Donor cells
Accumulated with oAβ
D
Cells with TNTs (%)
***
***
100
80
60
40
20
0
Acceptor cells no oAβ
Acceptor cells
Donor cells
Accumulated with oAβ

Figure 8

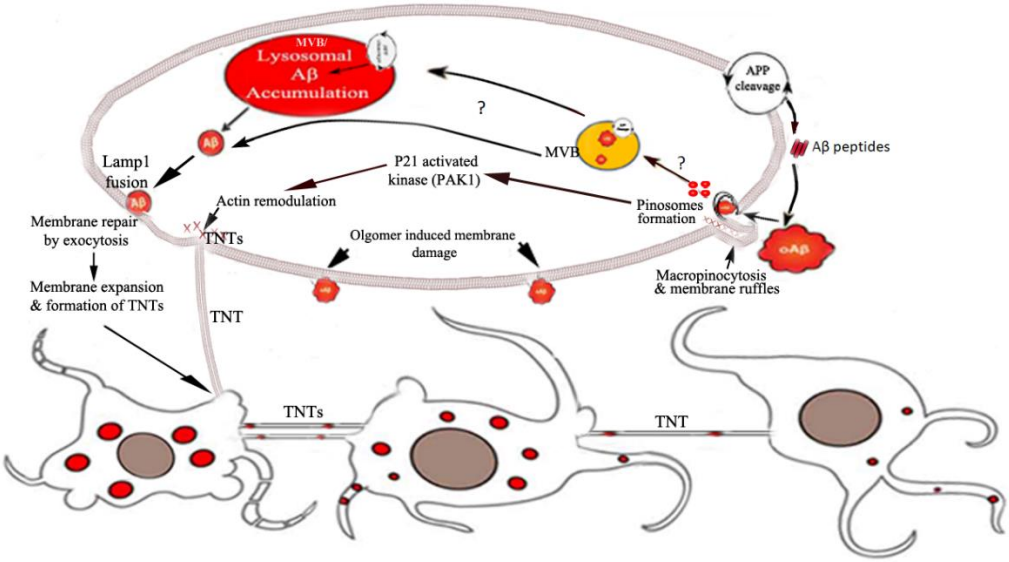
MVB/
Lysosomal
Aβ
Accumulation
APP
cleavage
Aβ peptides
?
MVB
?
Lamp1
fusion
P21 activated
kinase (PAK1)
Actin remodulation
Pinosomes
formation
Membrane repair
by exocytosis
TNTs
Olgomer induced membrane
damage
oAβ
Macropinocytosis
& membrane ruffles
Membrane expansion
& formation of TNTs
TNT
TNTs
TNT